AECL-7805

ATOMIC ENERGY OF CANADA LIMITED

L'ENERGIE ATOMIQUE DU CANADA, LIMITEE

THERMAL PROPERTIES OF CLAY-BASED BUFFER MATERIALS FOR A NUCLEAR FUEL WASTE DISPOSAL VAULT

PROPRIETES THERMIQUES DES MATERIAUX TAMPONS A BASE D'ARGILE POUR UNE ENCEINTE D'EVACUATION DES DECHETS DE COMBUSTIBLE NUCLEAIRE

H. S. Radhakrishna*

*Ontario Hydro

Whiteshell Nuclear Research Establishment

Etablissement de recherches nucléaires de Whiteshell

Pinawa, Manitoba R0E 1L0

June 1984 juin

ATOMIC ENERGY OF CANADA LIMITED

THERMAL PROPERTIES OF CLAY-BASED BUFFER MATERIALS FOR A NUCLEAR FUEL WASTE DISPOSAL VAULT

by

H.S. Radhakrishna*

* Ontario Hydro, Research Division

Whiteshell Nuclear Research Establishment
Pinawa, Manitoba ROE 1LO
1984 June

AECL-7805

PROPRIÉTÉS THERMIQUES DES MATÉRIAUX TAMPONS À BASE D'ARGILE POUR UNE ENCEINTE D'ÉVACUATION DES DÉCHETS DE COMBUSTIBLE NUCLÉAIRE

par

H.S. Radhakrishna*

RÉSUMÉ

On a fait l'étude des propriétés thermiques de trois types d'argiles à la bentonite, d'un schiste argileux riche en illite et d'un kaolin mélangé à du granite concassé. On fait des mesures de conductivité thermique pour une série de différentes proportions de mélange, de teneur en humidité, de densité et de température ambiante en employant la méthode de la sonde thermique transitoire. On a étudié les effets d'un séchage thermiques dans la zone de tampon avant l'absorption d'eau, par des essais au réchauffeur, à l'échelle du laboratoire. Le schiste riche en illite (Sealbond) et le kaolin ont présenté une meilleure compactabilité et une meilleure conductivité thermique que les argiles à la bentonite. La conductivité de tous les types d'argiles tampons dépendait à un degré élevé de l'humidité et n'avait relativement pas été affectée par une température élevée dans des conditions de pression élevée du fluide. Les matériaux tampons à la bentonite compactés à une densité sèche de 1200 à 1400 kg/m^3 ont eu de nombreuses fissures dues au retrait différentiel. L'addition de granite concassé et/ou le compactage à une densité plus élevée a réduit la fissuration thermique du matériau tampon.

* Ontario Hydro

L'Énergie Atomique du Canada, Limitée
Établissment de recherche nucléaires de Whiteshell
Pinawa, Manitoba ROE 1LO
1984

AECL-7805

THERMAL PROPERTIES OF CLAY-BASED BUFFER MATERIALS FOR A NUCLEAR FUEL WASTE DISPOSAL VAULT

by

H.S. Radhakrishna*

ABSTRACT

The thermal properties of three types of bentonite clay, one illite-rich shale and one kaolin mixed with crushed granite were investigated. Thermal conductivity measurements were made over a range of mix proportions, moisture content, density and ambient temperature using the transient heat-probe method. The effects of thermal drying in the buffer zone prior to water uptake were investigated by means of laboratory-scale heater experiments. Illite-rich shale (Sealbond) and kaolin exhibited better compactability and thermal conductivity than the bentonite clays. The thermal conductivity of all types of clay buffers showed a high degree of moisture dependency and relatively no effect due to elevated temperature under high fluid pressure conditions. Bentonite buffers compacted to a dry density of 1200 to 1400 kg/m^3 showed extensive cracking due to differential shrinkage. Addition of crushed granite, and/or compaction to a higher density, reduced the thermal cracking of the buffer material.

* Ontario Hydro

Atomic Energy of Canada Limited
Whiteshell Nuclear Research Establishment
Pinawa, Manitoba ROE 1LO
1984 June

AECL-7805

CONTENTS

1. INTRODUCTION

Safe and permanent disposal of nuclear fuel waste requires isolation of a number of diverse chemical elements from the environment for a long period of time. The Canadian concept for nuclear fuel waste disposal is to emplace the waste, packaged in corrosion-resistant containers, in a vault mined deep into plutonic rock in the Precambrian Shield [1]. This underground disposal vault will consist of a number of chambers, approximately 1000 m below the surface, interconnected by a system of tunnels and access shafts, as described in conceptual design reports by Acres Consulting Services Ltd. [2,3]. In the Canadian concept, the waste containers will most likely be placed in boreholes, about 4.7 m deep, drilled into the floor of the chambers, as shown in Figure 1. The annular space between the host rock and the container will be filled with a suitable material, called the 'buffer'.

An alternative to the borehole emplacement concept is the room emplacement concept, in which the containers will be embedded in a buffer mass within rooms or caverns, also shown in Figure 1.

After disposal operations have been completed, the design criteria require backfilling and sealing of the entire vault in such a manner as to isolate any harmful chemical elements that may be released from the waste due to natural breakdown of the containers.

The buffer, an engineered barrier, is required to perform the following functions: buffer the chemistry of the groundwater to enhance the life of the container; retard the migration of radionuclides if they are released from the waste form; provide mechanical support to the container and absorb any excessive stresses induced by movements of the surrounding rock; and dissipate the heat generated by the waste form, in the process of its decay, to the surrounding rock mass.

The physical and chemical attributes that the buffer material should possess to perform the aforementioned functions effectively over a long period of time were discussed in detail by Bird [4]. A research program to develop suitable buffer materials has been outlined by Bird and Cameron [5].

The work described in this report deals with the thermal characteristics of a selected list of buffer materials. The objective of this study was to evaluate the thermal properties of these candidate materials as potential buffers and to assess the heat-transport mechanism and the associated moisture migration phenomenon in the buffer. The results of this work will supplement these from other work in the buffer development program, to enable a selection of appropriate materials and installation techniques.

Previous work on buffer materials included thermal conductivity measurements in 1980 of clay-sand mixtures with clay contents ranging from 10 to 25% by dry weight. The material tested included

- o Black Hills Bentonie (sodium enriched) (BB)
- o Avonlea Bentonite (sodium enriched) (AVB)
- o Kaolin (K)
- o Sealbond (illite-rich shale) (SB)
- o Zeolite (Z)

all of which were mixed with graded silica sand (GS). The results of these tests are summarized in reference 6.

In 1981 the following clay materials, mixed with varying proportions (50 to 75%) of crushed granite, were tested:

- o Black Hills Bentonie (sodium enriched)
- o Avonlea Bentonite (sodium enriched)
- o Pembina Bentonite (sodium enriched)
- o Sealbond (illite-rich shale) and
- o Kaolin

Tests were also carried out on these clays with no crushed granite added.

The grain-size distribution curves for the individual components are shown in Figure 2. The physical properties of these materials are summarized in Table 1 and the chemical compositions of the clays are given in Table 2.

The crushed granite (2-mm size) used in this study was produced from the granite of the Lac du Bonnet batholith near Pinawa, Manitoba. This rock outcrop is considered to be similar in geochemical composition to the rock at depth. The results of the detailed chemical analysis of this rock are described in reference 7.

2. TESTING PROGRAM

The main objective of this study was to characterize the thermal properties of the candidate materials and to evaluate their performance under the thermal drying environment that would exist in the near field of the disposal vault. The test program was designed accordingly to determine the thermal conductivity of each candidate material as a function of clay percentage, moisture content, density and temperature.

The effects of moisture migration on the thermal conductivity of the buffer materials and the rates of thermal drying were evaluated by conducting a heater experiment. In these experiments different sized heaters were installed in large-diameter specimens (200 mm diameter, 300 mm long), and the thermal regime was monitored.

In the following sections a description of the test procedures and a discussion of the test results are given.

2.1 SPECIMEN PREPARATION

The crushed granite-clay mixtures were blended in their air-dried condition in proper proportions by dry weight, and then mixed with tap water in a Hobart mixer to produce a homogeneous material. The water was added gradually in a spray form while the material was being continuously mixed. The mixed material was then sealed in air-tight double plastic bags and stored for 2 d to allow the moisture to redistribute uniformly before compaction was done.

2.2 DYNAMIC COMPACTION

The mixed materials were compacted in three layers in steel moulds (102 mm diameter and 115 mm high)* using a 2.49-kg hammer free falling 305 mm. Each layer was compacted with 25 blows, according to ASTM procedure D698-78 [8]. In a few cases the materials were compacted in the same size moulds, but with a higher compaction energy (4.54-kg hammer free falling 457 mm) utilizing five layers. In this method, designated as 'modified Proctor compaction', the compaction energy is approximately four and one-half times that of the standard Proctor test [8]. The purpose of using the modified Proctor compaction method was to examine the effect of increased compaction effort on the density of the buffer specimens.

The moisture-density relationships for the various mixes tested are summarized in Figures 3 and 4. A summary of the specimen density, porosity and degree of saturation achieved for different mix compositions is given in Tables 3 to 5. Figure 5 shows the mixed materials and the compacted specimens.

2.3 STATIC COMPACTION

A few specimens were prepared by static compaction in a large-sized (150 mm diameter by 450 mm high) and heavy-walled split mould, which was bolted together to house a three-piece metal liner tube (see Figure 6). This arrangement facilitated removal of the compacted specimen from the mould for testing. The mould was designed for a maximum bursting pressure of 50 MPa. A thermal conductivity probe was positioned in the centre of the mould by clamping it into the base plate of the mould (Figure 6). A 6-mm diameter by 250-mm long probe was used. The specimen was compacted in 50-mm thick layers to a required density or under a specified compaction pressure. A micrometer dial gauge was used to control the thickness of each compacted layer. The static compaction was done in a 50-t capacity hydraulic press. Specimens with a diameter of 100 mm were also statically compacted in this mould by using filler blocks.

2.4 THERMAL CONDUCTIVITY MEASUREMENTS

The thermal conductivity of solids and particulate materials is normally determined by either the steady-state or the transient heat

---

* Because a large number of test specimens was required in this program, a split mould was used, and this was stripped from the specimens after compaction. The split mould was strapped with high-strength clamps to give it strength and stability during compaction.

dissipation method. The steady-state method has the disadvantage that errors occur in the measurements due to moisture migration in the direction of thermal gradients in moist soils and the potential for creating convection currents in saturated soils. Furthermore, the steady-state technique is time consuming.

The transient heat dissipation method (used in this study) is generally free of the above disadvantages. The measurement technique is relatively simple and fast, and is, therefore, favoured for the routine measurement of the thermal conductivity of particulate materials. In the transient heat dissipation method, a slender probe, simulating a line heat source, is inserted into the test specimen and the temperature rise of the probe is monitored over a period of 15 min with a constant heat input. The slope of the straight line portion of the temperature versus log-time plot is used to calculate the thermal conductivity of the material. The thermal conductivity, k, of the test material is calculated as follows:

$$k = \frac{2.303\ W \log_{10}(\frac{t_2}{t_1})}{L(T_2-T_1)} \qquad (1)$$

where W = input thermal power for the probe, in watts

L = length of the probe, in metres

T_1 and T_2 = temperature of the probe (°C) at times t_1 and t_2, respectively.

A microprocessor-based instrument was used to control the constant rate of heat input to the specimen, to collect temperature data at specified time steps and to fit a straight line to the data points, using the least-squares technique. Figure 7 illustrates the logic diagram for this thermal property analyzer.

The testing procedure consisted of inserting the thermal probe into the test specimen (102 mm diameter by 115 mm high) and allowing the probe to reach thermal equilibrium with the specimen before taking a measurement of the thermal conductivity. The test specimen was wrapped in a thin plastic sheet to prevent moisture evaporation during the test. Then the specimen was either dried in stages, with a thermal conductivity measurement at each equilibrium moisture level, or it was completely dried to zero moisture content (in an oven at 105°C) in a single stage, with a final measurement of the thermal conductivity of the dry specimen. The results of the single-stage drying tests are summarized in Table 6 and 7.

3. COMPACTABILITY OF CANDIDATE MATERIALS

The compaction characteristics of the crushed granite-clay mixtures were investigated, for each clay type, as a function of moisture content (m/c) and percentage clay in the mix. The dry density versus moisture content curves obtained from the standard and modified Proctor compaction

methods show (Figures 3 and 4) an increase in the achievable dry density as the clay content is reduced from 100% to 25% by dry weight. Kaolin and Sealbond exhibited superior compaction characteristics to the bentonite clays (Table 3). They also yielded lower porosities, higher degrees of saturation and lower optimum moisture contents than the bentonite clays. These are regarded as desirable attributes for stable thermal properties.

Among the three bentonite clays, the Black Hills Bentonite exhibited the highest optimum dry density of 1230 kg/m^3 at the lowest optimum moisture content of 33.4%. This was followed by the Avonlea Bentonite.

By increasing the compaction energy to about 4.5 times the standard Proctor energy, a significant increase in optimum density was achieved at a lower optimum moisture content (Figure 4). Optimum dry densities of 1520 kg/m^3 for Black Hills Bentonite, 1315 kg/m^3 for the Avonlea Bentonite and 1200 kg/m^3 for the Pembina Bentonite were obtained using the modified Proctor compaction energy.

Static compaction provided a better control of density than the dynamic compaction technique. The achievable dry density of the test specimens was limited by the maximum static pressure to 50 MPa for which the large compaction mould and the press were built. However, the practical limit for the static compaction setup was only 35 MPa, beyond which the elastic rebound of the mould and the sample produced horizontal cracking, resulting in poor density control.

Additional static compaction trials were carried out in a smaller size (100 mm diameter by 50 mm high), thick-walled stainless-steel mould to examine the relationship between achievable specimen density and static compaction pressure. The results of these tests on 100% clays are summarized in Figure 8. For all the clays tested, an increase in the compaction pressure above 50 MPa produced no significant increase in the dry density. Only the Black Hills Bentonite increased in density, from 1590 kg/m^3 to 1765 kg/m^3, by increasing the compaction pressure from 35 MPa to 50 MPa, beyond which there was no increase in density. Sealbond compacted to a high density of 2050 kg/m^3 under a static pressure of 35 MPa. The density for the Avonlea and Pembina Bentonites remained fairly constant at an average value of 1550 ± 30 kg/m^3 for compaction pressures between 35 and 65 MPa.

Pusch, in his buffer study, achieved a dry density in the range of 1900 kg/m^3 for 100% bentonite (similar in composition to Black Hills Bentonite) by means of isostatic compression under 50 MPa [9]. Very high compaction pressures would be required to produce similar densities by uniaxial compression. The equipment used in this study was not capable of producing the very high density samples.

From the above discussion it would appear that a practical limit for achievable density by in situ compaction would be 1500 kg/m^3 for 100% bentonite clays and 2000 kg/m^3 for mixtures of crushed granite and bentonite. For densities higher than these limits the buffer would have to be emplaced in the form of precompacted blocks, as proposed by Pusch [9].

In this study the test specimens were compacted to densities achievable by conventional compaction techniques, and thus the properties measured reflect these conservative limits.

4. THERMAL CONDUCTIVITY OF CANDIDATE MATERIALS

The thermal conductivity of candidate buffer materials was measured as a function of (i) clay type, (ii) clay content, (iii) dry density, (iv) moisture content and (v) temperature.

Tables 6 and 7 illustrate the range of thermal conductivity values for crushed granite-clay mixtures containing different clay types: Black Hills Bentonite (BB), Avonlea Bentonite (AVB), Pembina Bentonite (PB), Sealbond (SB), Kaolin (K), and having different clay proportions (25, 50, 75 and 100% by dry weight). The moisture content and density values indicated are the limits within which the thermal conductivity measurements were made.

4.1 EFFECT OF CLAY TYPE AND CLAY CONTENT

The thermal conductivity of the compacted crushed granite-clay mixes generally decreased with an increase in clay content (Figure 9). This trend was most pronounced in the case of Black Hills Bentonite, and to a lesser degree in the case of Sealbond and Kaolin. The bentonite-based mixes exhibited the lowest thermal conductivity values for all of the mix proportions. This behaviour is partly due to the low interparticle density and poor conductance at the interparticle contacts.

4.2 EFFECT OF MOISTURE CONTENT

The moisture dependency of the thermal conductivity of the bentonite- and Sealbond-based buffers is shown in Figures 10 and 11. A significant drop in the thermal conductivity (by about 50%) at moisture contents below 5 to 10% (by dry weight) is indicated by these tests. The specimens compacted under a static load also exhibited similar behaviour with respect to moisture content (see Figure 12). The initial conditions of the test specimens are summarized in Table 7.

4.3 EFFECT OF DENSITY

The density dependence of the thermal conductivity of the bentonite- and Sealbond-based buffers is shown in Figure 13. This plot shows that significant improvements in the thermal conductivity of clay-based buffers can be achieved by increasing their interparticle density, and/or by adding coarse-grained fractions such as silica or crushed granite. Among the bentonites obtained from the three sources (Black Hills, Avonlea, and Pembina), Black Hills Bentonite had the highest thermal conductivity for a comparable dry density.

The addition of crushed granite in an equal proportion to the clay (viz, CGBB-50) significantly improved both the density and the thermal conductivity. A buffer mix containing only 25% crushed granite and 75% Black Hills Bentonite (CGBB-75), however, did not show any improvement in the dry thermal conductivity in comparison to the 100% Black Hills Bentonite (BB-100).

It was also observed that the degree of shrinkage and cracking upon drying was essentially the same (moderate) for the bentonite specimens

containing 0% and 25% crushed granite, whereas for those containing 50% crushed granite the cracking was minimal. It would, therefore, appear that addition of only 25% crushed granite (filler material) is not adequate to enhance the dry thermal conductivity of the Black Hills Bentonite when compacted under standard Proctor energy.

4.4 EFFECT OF AMBIENT TEMPERATURE

In the Canadian reference design for a nuclear fuel waste vault, the near-field ambient temperature is estimated to be approximately 100°C for several years following waste emplacement [2,3]. In the early stages of the vault's life, it is probable that the hydrostatic pressure in the buffer mass will not be sufficient to suppress significantly the boiling point of the pore water, in which case the moisture in the buffer may migrate in the vapour phase. Over the long term, however, the buffer mass will become resaturated and the hydrostatic pressure will eventually be adequate to suppress boiling of the pore water.

To investigate the effect of a high ambient temperature on the thermal conductivity of the buffer material, experiments were conducted in which the test specimens were sealed against vapour loss and placed in a constant high-temperature environment. The thermal conductivity measurement was performed in the standard manner after the specimen reached thermal equilibrium. The ambient temperature and the interior temperature of the specimen were monitored during the thermal conductivity measurements to ensure that the ambient temperature remained constant during the test. The thermal probe and the lead wires were designed to withstand a temperature of 200°C.

Two sets of tests were performed. In the first set, the samples were sealed but not pressurized, whereas in the second set the samples were subjected to 200 kPa of nitrogen pressure, which is sufficient to suppress pore water boiling under an ambient temperature of 120°C. The test setup used is shown in Figure 14. The initial and final conditions of the test specimens are summarized in Table 8.

The thermal conductivity of the buffer samples did not show a strong dependence on the ambient temperature, up to 100°C (see Figure 15). At higher temperatures the samples that were vapour sealed, but not pressurized, showed a drop in their thermal conductivity. This trend was accompanied by shrinkage and cracking in the case of the BB-100 sample (see Figure 16(a)). However, an identical sample, when pressurized to 200 kPa with nitrogen gas, exhibited only shrinkage but no cracking (see Figure 17(a)). Also the sample with 50% crushed granite exhibited very little cracking, even when the sample was not pressurized (see Figure 16(b)). In one of the test specimens of BB-100, moisture loss occurred due to a vapour leak in the mould assembly and, as a result, the specimen shrank and cracked severely, as shown in Figure 17(b).

Thus, the only effect of high ambient temperature on the thermal properties of clay-based buffers would be that of moisture loss in the vapour phase. If vapourization of the soil moisture is prevented by high hydrostatic pressures, then the high-temperature environment should have no

significant effect on the thermal conductivity of the buffer. Tests conducted on sodium-enriched bentonite (similar in composition to Black Hills Bentonite) by Sandia National Laboratories confirms this observation [10]. In their test program they subjected densely compacted bentonite specimens (dry density = 2100 kg/m^3 and moisture content = 19%) to progressively increasing temperatures up to a maximum of 300°C. No significant change in thermal conductivity was observed for temperatures up to 100°C, above which the loss of moisture accounted for a decrease in thermal conductivity of about 20%.

From the above discussion it can be inferred that the thermal conductivity of the buffer mass exhibits a strong dependence on its moisture content and density, but to a lesser degree on ambient temperature. In selecting the buffer composition, the following factors should be considered:

(1) Bentonite-based materials have lower thermal conductivities than Sealbond and Kaolin.

(2) Black Hills Bentonite is marginally superior to the Avonlea and Pembina Bentonites in its compactability and thermal conductivity properties.

(3) Additions of crushed granite, in proportions of not less than 50%, improve compactability and thermal conductivity, and result in reduced shrinkage cracking upon drying.

(4) Increasing the compaction energy to achieve dry densities of 2000 kg/m^3 for clay-granite mixtures offers improved thermal conductivity and minimal shrinkage cracking upon drying. If the moulding moisture is kept very low (a Swedish researcher used air-dried bentonite at 8% moisture content [9]), much of the thermal cracking during initial periods of drying can be eliminated.

5. HEATER EXPERIMENTS

In the early stages of a nuclear fuel waste vault's life, after the waste has been emplaced and backfilled, the unsaturated buffer mass will be exposed to thermal gradients in the proximity of the waste containers. If the influx of water from the host rock is slow, then there is a possibility that the buffer mass may dry out by moisture migration. A similar process in an underground power cable backfill, termed a 'thermal runaway' condition, leads to cable failure due to overheating. However, in the case of radioactive waste containers, no such concern exists. Instead, the integrity of the buffer mass and the host rock is of major concern.

An experiment was devised to examine the effects of thermal drying on the performance of the buffer materials by embedding a heater in a large test specimen (200 mm diameter by 300 mm high) and supplying a constant heat input (Figure 18). The thermal regime in the radial direction was continuously monitored by thermocouples in the heater and also at various locations within the specimen (Figure 19).

Two sizes of heaters (6.35 mm and 25.4 mm in diameter) were used to vary the heat flux at the heater-soil contact. The smaller diameter heater was equipped with one thermocouple, which was embedded inside the heater. The larger diameter heater was provided with two thermocouples, one embedded inside the heater and the other one on the metal sheath, in contact with the soil.

The test specimen was then placed within a 1.8-m x 1.8-m x 0.5-m block of fly-ash concrete, to simulate a host rock of medium thermal conductivity [2.0 W/(m•°C)], and the annular space was packed with the buffer material (Figure 18). The top and bottom ends were insulated against heat loss by means of rigid styrofoam boards, to simulate radial heat flow from a cylindrical heat source.

Test specimens of the various buffer materials were manually compacted in layers in a split mould, either to the optimum or a specified density. The heater was positioned in the centre of the mould by fastening it to the base plate, and the specimen was then compacted around it in thin lifts. This procedure ensured uniform density and moisture distribution throughout the specimen. Table 9 summarizes the initial conditions of the test specimens. Tests were conducted on the BB-100 and CGBB-50 mixes only, as these mixes were identified as the ones that exhibited the greatest effects due to thermal drying.

In these tests the size of the heater and the buffer zone were not scaled to simulate the near-field conditions of an actual disposal vault. Instead, the experiments were designed to accelerate the process of thermal drying and to evaluate the performance of the buffer materials on this basis. The following comparison between the conditions in the test and those in the near field of a disposal vault will illustrate this point:

Parameter	Experiments	Typical Waste Container Parameters [2,3]	
		Borehole Case	In-Room Case
Heater Diameter	6.35 or 25.4 mm	457 mm	910 mm
Heater Length	0.3 m	3.03 m	1.5 m
Length/Diameter Ratio	48 or 12	6.6	1.6
Heat Flow	Radial	3-Dimensional	3-Dimensional
Heat Input	100 W/m	100 W/m	200 W/m
Heat Flux at Heater-Buffer Interface	5000 to 1250 W/m^2	70 W/m^2	70 W/m^2
Duration	7 d	100 to 1000 a	100 to 1000 a

The selection of the test parameters was based on Hartley and Black's drying time theory [11,12] in which they postulated that, for an infinitely long cylindrical heat source, the drying time at which a thermal instability will develop due to the onset of soil moisture migration can be scaled as follows:

$$t_p = t_s \left(\frac{D}{d}\right)^2 \qquad (2)$$

where t_p = drying time for the full-scale heat source (waste container in this case)

t_s = drying time for the scaled heater used in the experiment

D = diameter of the full-scale heat source

d = diameter of the experimental heater.

Even though this model was verified in the experiments of Hartley and Black [11], the boundary effects were not fully investigated. In the present series of experiments, the specimen size and the encapsulating block of fly-ash concrete were sufficiently large to allow the experiment to continue for about one week without being affected by the boundary conditions.

Three samples of BB-100 and two samples of CGBB-50 were tested. The test data are summarized in Table 9. Two specimens of both BB-100 and CGBB-50 were manually compacted with a heater embedded within them. One specimen of BB-100 was statically compacted in a hydraulic press.

The temperature distribution within the specimen and in the surrounding fly-ash concrete block was monitored continuously over the test duration. The temperature-time data obtained are shown in Figures 20 to 24. The difference between the temperature of the heater sheath and that of the soil in contact with the heater represents the effect of contact resistance.

Figure 25 shows the radial temperature distribution in the specimen for different test runs. A linear relationship between soil temperature and log-distance represents a uniform thermal conductivity in the radial direction. A non-linearity or sudden change in slope indicates moisture migration due to thermal drying. Figure 25 shows that there is moisture migration in the vicinity of the heater in all of the test cases.

The moisture distributions throughout the specimens after the test, in both the vertical and radial directions, are shown in Figure 26. The specimen conditions after completion of the tests are shown in Figures 27 to 31.

The following observations were made from the results of these tests.

5.1 THERMAL INSTABILITY

(1) In all of the tests the temperature versus log-time curves exhibited deviation from a linear relationship somewhere between 60 to 200 min, indicating a definite decrease in the thermal

conductivity (k) by as much as 50% at the heater-soil interface (Figures 20 to 24). (The lag between the internal and external tempertures of the heater is due to the thermal properties of the heater.)

In the case of the statically compacted specimens of BB-100 and the dynamically compacted specimens of CGBB-50 (Figures 22 to 24), the changes in the shape of the temperature-time curve were more gradual than in the other BB-100 specimens (Figures 20 and 21).

(2) The break point in the linear relationship between the temperature versus log-time curve is called the initial drying time. The initial drying times obtained from these tests (Table 8) did not support Hartley and Black's theory [11,12] for scaling of the initial drying time from one size of heat source to another. The initial drying time for the 25.4-mm diameter heater was either equal to or less than that for the 6.35-mm diameter heater with all the other factors (sample conditions and heat input) being the same.

Since thermal instability was evident in all the experiments, the scaling of drying times from these experiments to that for a waste container-buffer system is not considered practical.

(3) Comparing the temperature profiles in the radial direction at the initial drying time for the different test runs (Figure 25) indicates that the specimens with a smaller diameter (6.2 mm) heater experienced thermal gradients three to four times greater than those in identical specimens having a larger diameter (25.4 mm) heater.

(4) A statically compacted bentonite specimen showed a somewhat more stable thermal regime, which was indicated by a more uniform temperature gradient across the specimen (Figure 25). This was accompanied by uniform drying throughout the specimen, as indicated by the soil moisture profile determined at the end of the test (Figure 26).

(5) With the exception of the statically compacted bentonite specimen, a zone of thermal drying was evident from the final moisture content determinations (Figure 26).

(6) Except in the case of the statically compacted bentonite specimen, the rate of temperature rise within the test specimen gradually decreased after about 1000 min, while the temperature at the heater-soil interface increased at a faster rate. This is attributed to sample inhomogeneity caused by moisture migration and shrinkage cracking.

5.2 SHRINKAGE AND CRACKING

Clay-based materials are known to exhibit shrinkage and cracking during the process of drying, especially if the drying is non-uniform and progresses from one region to another. In the heater experiments, a high thermal gradient was produced near the heater, as shown in Figure 25.

The test specimens exhibited various degrees of shrinkage cracking due to differential drying across the specimen. The cracks were predominantly in the radial direction and some extended through the full thickness of the specimens. The Black Hills Bentonite samples with no crushed granite cracked more than those with crushed granite (Figures 27 to 31). Also, the statically compacted specimen, which had the highest density (1555 kg/m^3) among the three bentonite samples tested, showed the least amount of cracking (Figure 31). Thus, a high-density material with a coarse-grained fraction will be necessary if cracking due to thermal drying is to be minimized.

The published data on highly compressed bentonite suggest that very little or no cracking occurs due to thermal drying if the bentonite is compacted to densities greater than 2000 kg/m^3, at low moisture contents (7 to 10%) [10].

In view of the results of the heater experiments, it is suggested that the buffer material should be compacted to a dry density of at least 1600 kg/m^3 in the case of the BB-100 material, and to a density of 1900 kg/m^3 in the case of the CGBB-50 material, to minimize cracking due to thermal drying.

6. CONCLUSIONS

From the results of various measurements of thermal conductivity and the heater experiments described above, the following conclusions can be drawn:

(1) The thermal conductivity of clay-based buffers is highly dependent on moisture content in the low moisture region and the relationship is generally nonlinear.

(2) The density to which a clay buffer is compacted affects its thermal conductivity. An addition of crushed granite or silica improves the thermal conductivity through improved compactability.

(3) The ambient temperature has no significant effect on the thermal conductivity of the buffer, provided the buffer moisture is not allowed to vapourize.

(4) Among the five clay types tested, the Kaolin and Sealbond materials exhibited superior thermal conductivities to the bentonites. In its totally dried state, a bentonite buffer has a thermal conductivity in the range 0.4 to 0.5 W/(m•°C).

(5) Among the three bentonites tested (Black Hills, Avonlea and Pembina), Black Hills Bentonite (sodium enriched) exhibited the most superior compaction characteristics and also had the best thermal conductivity.

(6) In the case of both the borehole and room-emplacement concepts, the buffer material will most likely dry out under the sustained thermal gradients prior to the natural reflooding of the vault. During this thermal drying phase, the buffer material will experience cracking due to differential shrinkage. The degree of cracking will depend on the placement density and moisture content of the buffer material.

(7) For a bentonite buffer, a dry density of 1600 kg/m^3 or higher should be achieved at as low a moisture content as possible (less than its optimum moisture content) to minimize shrinkage cracking during the initial thermal drying phase.

(8) Addition of a coarse-grained material, such as sand or crushed granite, to a bentonite buffer material will reduce the extent of cracking. A buffer mix with equal proportions of crushed granite and bentonite will have good thermal conductivity and minimal shrinkage and cracking when compacted to a dry density of 1900 kg/m^3, or greater.

A full-scale heater experiment for the final selected buffer material, simulating the various hydrothermal phases in the disposal vault's life, would appear to be necessary to evaluate the effects of sustained thermal gradients and moisture movements.

REFERENCES

1. J. Boulton (Editor), "Management of Radioactive Fuel Wastes: The Canadian Disposal Program," Atomic Energy of Canada Limited Report, AECL-6314 (1978).

2. Acres Consulting Services Ltd. and Associates, "A Disposal Centre for Irradiated Nuclear Fuel: Conceptual Design Study," Atomic Energy of Canada Limited Report, AECL-6415 (1979).

3. Acres Consulting Services Ltd. and Associates, "A Disposal Centre for Immobilized Nuclear Waste: Conceptual Design Study," Atomic Energy of Canada Limited Report, AECL-6416 (1979).

4. G.W. Bird, "Possible Buffer Materials for Use in a Nuclear Waste Vault," Atomic Energy of Canada Limited Technical Record*, TR-72 (1979).

5. G.W. Bird and D.J. Cameron, "Vault Sealing for the Canadian Nuclear Fuel Waste Management Program," Atomic Energy of Canada Limited Technical Record*, TR-145 (1982).

6. H.S. Radhakrishna, "Evaluation of the Thermal Properties of Buffer Materials for a Deep Underground Nuclear Waste Disposal Vault," Atomic Energy of Canada Limited Technical Record*, TR-183 (1982).

7. "Analysis of Surface Outcrop Rocks in the Lac du Bonnet Batholith, Field Samples 1977," Atomic Energy of Canada Limited Technical Record*, TR-20 (1979).

8. American Society for Testing and Materials, Annual Book of ASTM Standards, Part 19, Philadelphia, 1982.

9. R. Pusch, "Highly Compacted Sodium Bentonite for Isolating Rock Deposited Radioactive Waste Products," Nuclear Technology 45, 153 (1979).

10. J.G. Hartley and W.Z. Black, "Transient Simultaneous Heat and Mass Transfer in Moist, Unsaturated Soils," ASME J. of Heat Transfer 103, 376 (1981).

11. J.G. Hartley, W.Z. Black, R.A. Bush and M.A. Martin, "Measurements, Correlations and Limitations of Soil Thermal Stability," Proceedings of the Symposium on Underground Cable Thermal Backfill, September 1982, Toronto, Pergamon Press (1982).

---

* Unrestricted, unpublished report available from SDDO, Atomic Energy of Canada Limited Research Company, Chalk River, Ontario K0J 1J0.

TABLE 1

PHYSICAL PROPERTIES OF BUFFER MATERIALS TESTED

Component	Specific Gravity*	Size Fractions (%)			Air-Dried Moisture Content (%)	Liquid Limit**	Plasticity Index
		Sand	Silt	Clay			
Crushed granite	2.61	93	7	0	0.5	-	-
Black Hills Bentonite	2.74	0	13	87	6.8	501.0	462.0
Avonlea Bentonite	2.71	0	39	61	6.8	199.0	152.0
Pembina Bentonite	2.77	2	38	60	10.7	127.0	78.0
Sealbond	2.76	3	65	32	0.8	27.5	7.6
Georgia Kaolin	2.60	0	30	70	0.8	38.0	11.5

* Clay samples were presoaked with distilled water for 48 h before the specific gravity measurements were made, as per ASTM procedure D854-58.

** Clay samples were presoaked in distilled water for 96 h with water contents well above the liquid limit and then air dried in stages to lower the water contents. Liquid and plastic limits were determined as per ASTM Procedures D423-66 and D424-59, respectively.

TABLE 2

CHEMICAL COMPOSITIONS OF CLAY MATERIALS USED TO PREPARE BUFFER SPECIMENS

Material	Chemical Composition (%)*									Loss on Ignition (%)	pH
	SiO_2	Al_2O_3	Fe_2O_3	Mno	TiO_2	CaO	MgO	K_2O	Na_2O		
Black Hills Bentonite	65.0	20.2	2.3	1.0	0.1	1.4	1.0	0.8	3.1	7.0	8.4
Avonlea Bentonite	60.0	18	2.0	-	-	0.8	2.0	-	2.3	5.5	9.2
Pembina Bentonite	Chemical Composition Not Available From Supplier									21.3	?
Sealbond	58.5	16.0	7.3	0.1	0.9	3.4	-	4.2	0.8	4.1	?
Georgia Kaolin	45.1	38.1	0.6	-	1.4	Trace	0.2	0.1	0.3	13.8	5 to 7

* Chemical compositions provided by suppliers

TABLE 3

CLAY BUFFER MATERIALS
STANDARD PROCTOR COMPACTION RESULTS

Material Composition	BB-100*	AVB-100*	PB-100*	SB-100*	K-100*
Moisture Range (%)	26.7 - 59.6	26.2 - 61.4	42.2 - 64.2	10.3 - 21.5	11.4 - 41.2
Dry Density Range (kg/m^3)	980 - 1230	940 - 1125	925 - 1030	1665 - 1780	1195 - 1510
Porosity Range (%)	54.6 - 63.8	58.5 - 64.8	62.8 - 66.6	35.5 - 39.7	41.9 - 54.0
Degree of Saturation (%)	58.4 - 91.5	50.4 - 90.5	58.6 - 93.6	47.8 - 90.2	27.0 - 97.2
Optimum Moisture Content (%)	33.4	38.6	46.5	16.9	27.0
Optimum Dry Density (kg/m^3)	1230	1080	1030	1780	1510
Porosity at Optimum Moisture Content and Density (%)	54.6	60.1	62.8	35.5	41.9
Degree of Saturation at Optimum Moisture Content and Optimum Dry Density (%)	75.2	69.3	76.3	84.7	97.2
Specific gravity	2.71	2.71	2.77	2.76	2.60

* 100 = 100% Clay (no crushed granite admixture)

TABLE 4

CRUSHED GRANITE AND CLAY MIXTURES
STANDARD PROCTOR COMPACTION RESULTS

Property of Compacted Specimens	Material Composition					
	CGBB-50*	CGBB-25	CGSB-50	CGSB-25	CGK-50	CGK-25
Moisture Range (%)	13.1 - 53.6	11.0 - 18.4	9.3 - 14.7	6.8 - 11.7	8.8 - 14.7	5.7 - 11.0
Dry Density Range (kg/m^3)	970 - 1595	1630 - 1735	1810 - 1935	1925 - 2060	1705 - 1860	1805 - 2020
Porosity Range (%)	40.0 - 63.5	34.2 - 38.1	27.9 - 32.6	22.2 - 27.3	28.7 - 34.7	22.6 - 30.8
Degree of Saturation (%)	44.7 - 85.2	47.0 - 84.6	51.7 - 86.1	47.9 - 94.7	43.3 - 91.3	33.4 - 88.5
Optimum Moisture Content (%)	21.4	15.2	12.3	10.0	14.1	9.9
Optimum Dry Density (kg/m^3)	1595	1735	1935	2060	1860	2020
Porosity at Optimum Moisture Content and Density (%)	40.0	34.2	27.9	22.2	28.7	22.6
Degree of Saturation at Optimum Moisture Content and Optimum Dry Density (%)	85.2	77.2	85.1	92.9	91.3	88.5

* CGBB = Crushed Granite with 50% Black Hills Bentonite mix (on dry weight basis)

TABLE 5

SUMMARY OF MODIFIED PROCTOR COMPACTION TEST DATA FOR 100 PERCENT CLAY SPECIMENS

Property of Compacted Specimens	Material Composition		
	BB-100	PB-100	AVB-100
Moisture Range (%)	20.6-36.3	34.8-53.8	23.6-44.2
Dry Density Range (kg/m^3)	1341-1519	1089-1200	1200-1313
Porosity Range	43.9-50.5	56.7-60.7	51.5-55.7
Degree of Saturation Range (%)	61.8-96.3	83.2-96.1	55.6-95.2
Optimum Mositure Content (%)	25.4	42.3	34.5
Optimum Dry Density (kg/m^3)	1519	1200	1313
Porosity at Optimum Moisture Content and Density (%)	43.9	56.7	51.5
Saturation at Optimum Mositure Content and Optimum Density (%)	87.8	89.6	87.9

TABLE 6

SUMMARY OF THERMAL CONDUCTIVITIES OF CANDIDATE BUFFER MATERIALS

Mix Composition	Moisture Content Range (%)	Dry Density Range* (kg/m^3)	Thermal Conductivity in Moist Condition (W/(m·°C))	Thermal Conductivity in Dry Condition (W/(m·°C))	Extent of Cracking After Drying
BB-100	20 - 30	1200 - 1250	0.7 - 1.1	0.5 - 0.6	Moderate to Severe
CGBB-25	6 - 12	1620 - 1710	1.0 - 1.5	0.6 - 0.8	None
CGBB-50	12 - 17	1500 - 1550	0.8 - 1.2	0.5 - 0.6	Moderate
CGBB-75	18 - 25	1320 - 1450	0.8 - 1.0	0.4 - 0.6	Moderate to Severe
AVB-100	26 - 33	1050 - 1140	0.6 - 0.9	0.4 - 0.5	Severe
PB-100	35 - 45	1000 - 1120	0.8 - 1.2	0.4 - 0.5	Severe
SB-100	12 - 18	1500 - 1700	1.2 - 1.8	0.6 - 1.0	None to Moderate
CGSB-25	7 - 12	1600 - 2050	1.4 - 2.4	0.8 - 1.0	None
CGSB-50	9 - 15	1850 - 1980	1.8 - 2.4	0.9 - 1.0	None
CGK-25	9 - 12	1850 - 2000	1.7 - 2.5	0.9 - 1.2	None
CGK-50	9 - 15	1770 - 1860	2.0 - 2.2	1.0 - 1.2	None
K-100	25 - 35	1300 - 1500	1.2 - 1.6	0.7 - 1.0	Moderate

* Samples compacted according to ASTM procedure D698-78.

TABLE 7

THERMAL CONDUCTIVITY OF STATICALLY COMPACTED BUFFER SPECIMENS

Mix Composition	CGBB-50	CGBB-25	CGSB-50	BB-100
Maximum Compaction Pressure (MPa)	35	35	35	35
Moisture Content (%)	15.7	10.3	10.4	19.8
Dry Density (kg/m^3)	1882	2080	2107	1555
Porosity (%)	29.2	21.3	21.5	43.0
Degree of Saturation (%)	100	100	100	72.5
Thermal Conductivity (as Packed) ($W/(m \cdot °C)$)	1.60	2.10	2.32	0.80
Thermal Conductivity (Oven Dried at 105°C) ($W/(m \cdot °C)$)	0.86	1.20	1.00	0.56

TABLE 8

SUMMARY OF DENSITY AND MOISTURE CONDITIONS OF THE SAMPLES USED FOR STAGE DRYING AND HIGH-TEMPERATURE TESTS

Type of Test	Mix Composition	Initial Moisture Content (%)	Final Moisture Content (%)	Dry Density (kg/m^3)
Stage Drying	BB-100	19.4	0.6	1223
	CGBB-50	15.4	0.0	1636
	SB-100	13.1	0.0	1837
	CGSB-50	9.7	0.0	2009
High Ambient Temperature (Not Pressurized)	BB-100	20.0	5.9	1293
	CGBB-50	15.5	2.5	1650
	SB-100	12.8	9.0	1820
	CGSB-50	10.0	6.3	2020
	CGK-50	15.0	5.2	2105
High Ambient Temperature Pressurized with Nitrogen to 203 kPa (2 atm)	BB-100	39.5	31.2	1310
	PB-100	46.4	43.4	1015

TABLE 9

SUMMARY OF RESULTS FROM HEATER EXPERIMENTS ON CLAY-BASED BUFFERS

Mix Composition	Initial Moisture Content (%)	Dry Density (kg/m^3)	Sample Size		Heater Size		Heat Input (W/m)	Thermal Conductivity (W/(m·°C))		Final Moisture Content (%)		Initial Drying Time (min)
			Dia (mm)	Length (mm)	Dia (mm)	Length (mm)		Initial	Final	Core	Surface	
BB-100 Hand Compacted	19.5	1476	200	300	6.35	250	96.8	0.88	0.5	-	-	200
BB-100 Hand Compacted	19.9	1426	200	300	25.4	285	100.3	1.09	0.44	10	22	100
BB-100 Statically Compacted	19.5	1555	150	300	25.4	285	99.8	1.66	0.82	15	16	80
CGBB-50 Hand Compacted	13.9	1440	200	300	6.35	245	99.2	1.08	0.65	3	17	80
CGBB-50 Hand Compacted	13.5	1495	200	300	25.4	285	100.6	1.18	0.63	7	17	100

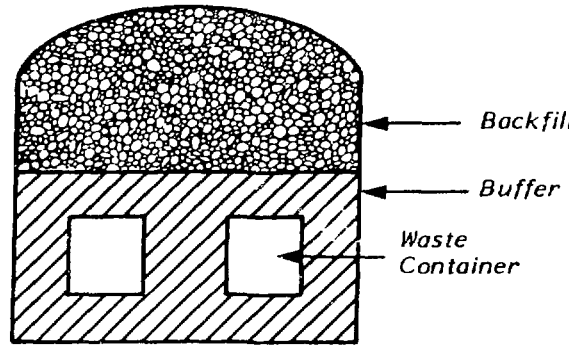

(a) In-Room Emplacement

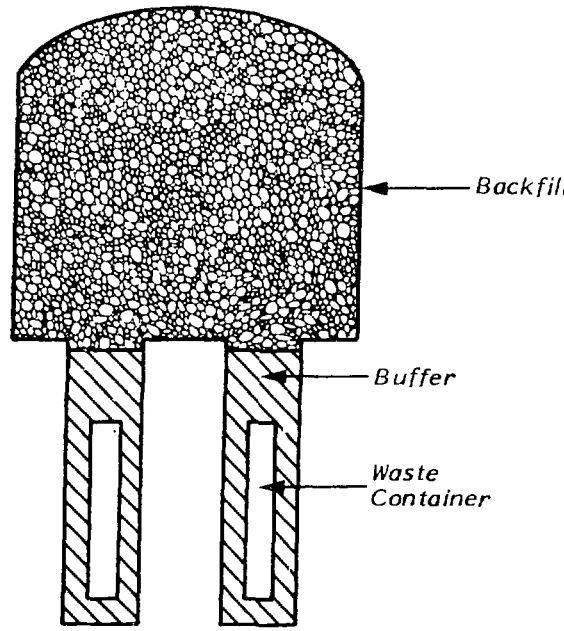

(b) Borehole Emplacement

FIGURE 1: Schematic Illustration of Two Methods of Nuclear Fuel Waste Disposal

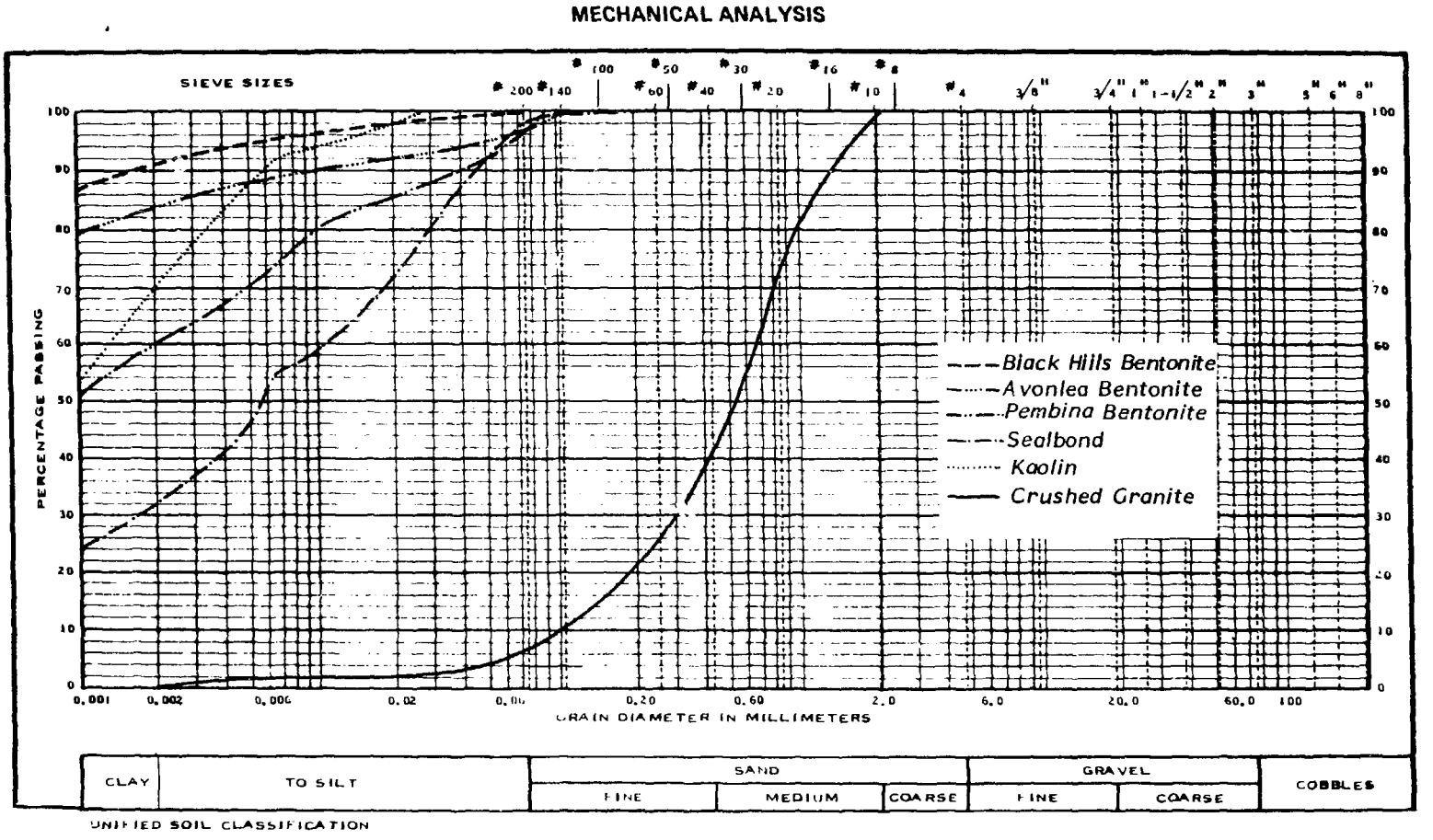

FIGURE 2: Grain Size Distribution Curves for the Fine and Coarse Fractions of Buffer Mixes

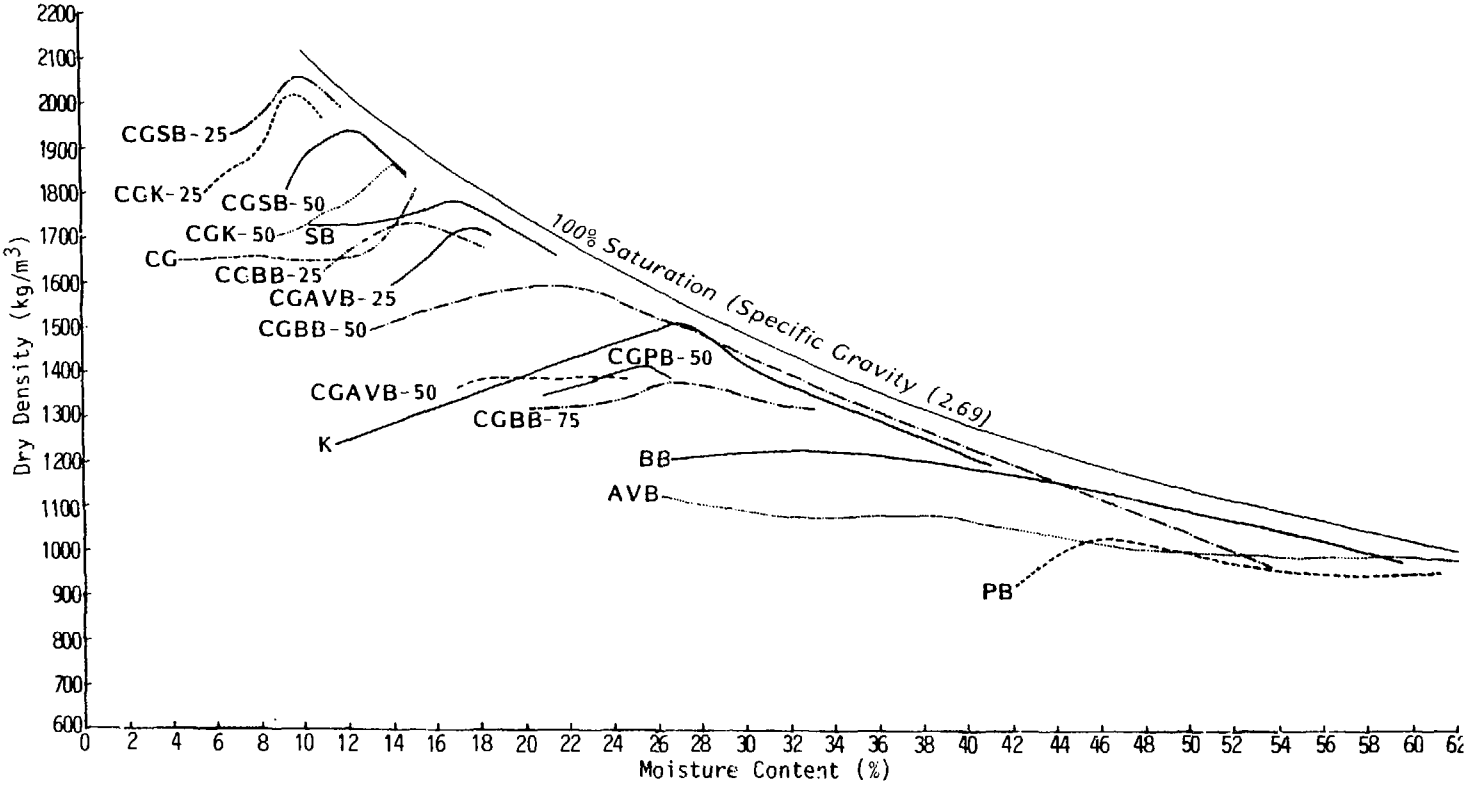

FIGURE 3: Summary of Standard Proctor Compaction Test Data on Clay-Based Buffers

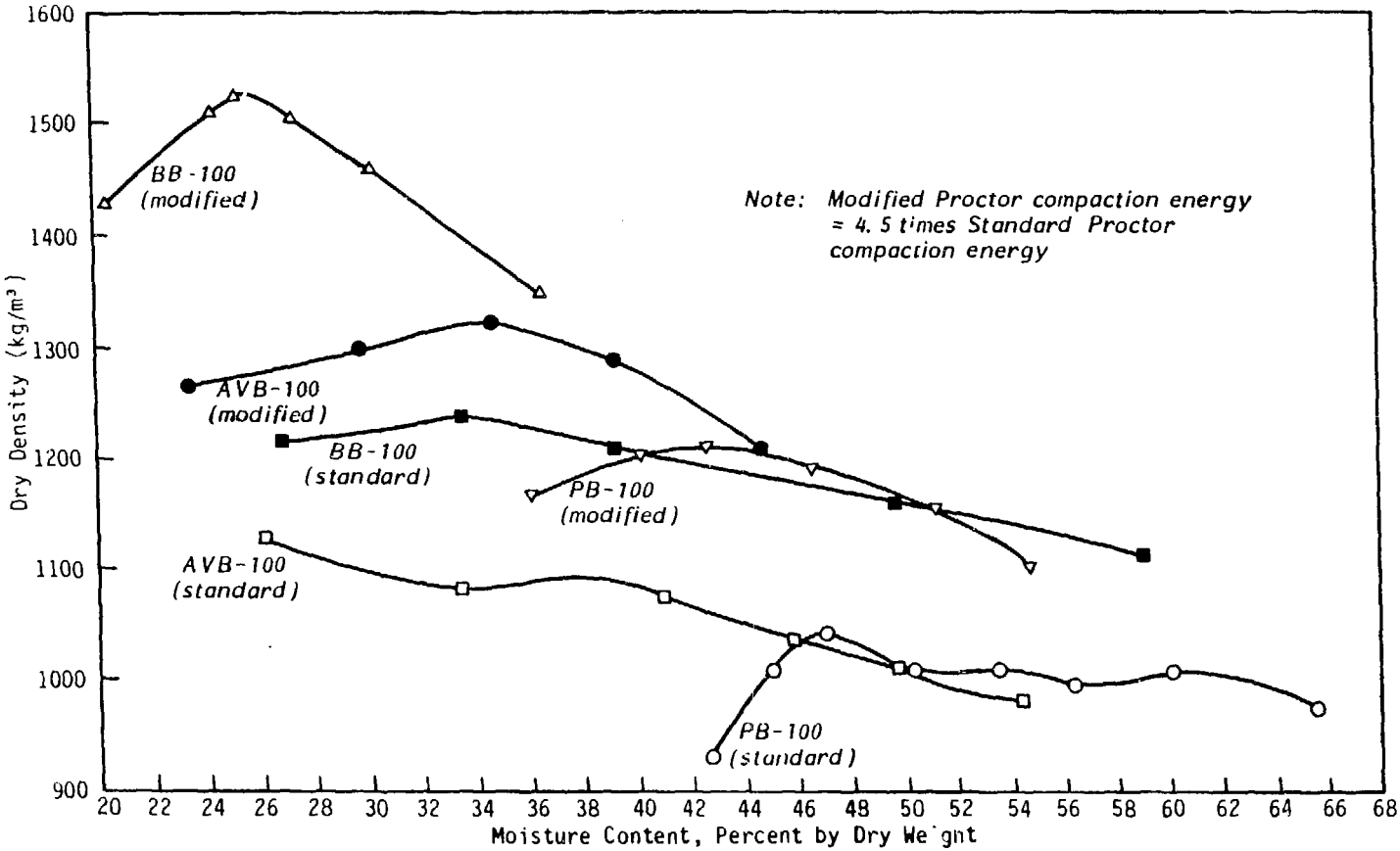

FIGURE 4: Standard and Modified Proctor Compaction Curves for Different Sources of Bentonite

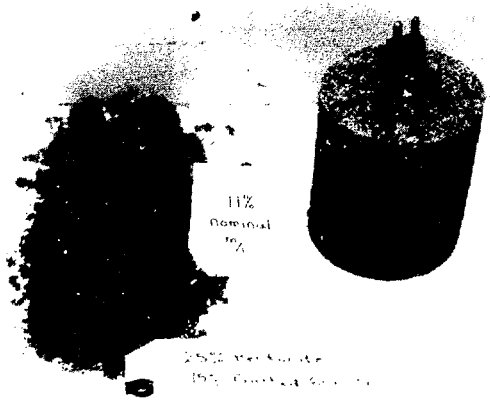

Crushed Granite + Bentonite
(75% + 25% mix)

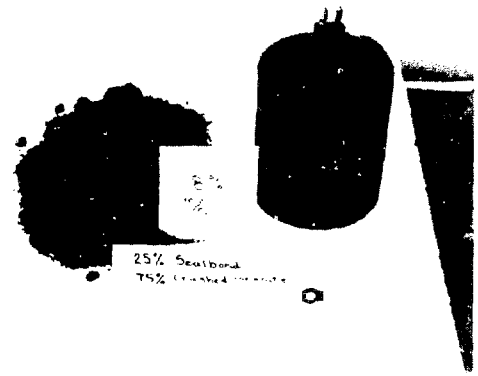

Crushed Granite + Sealbond
(75% + 25% mix)

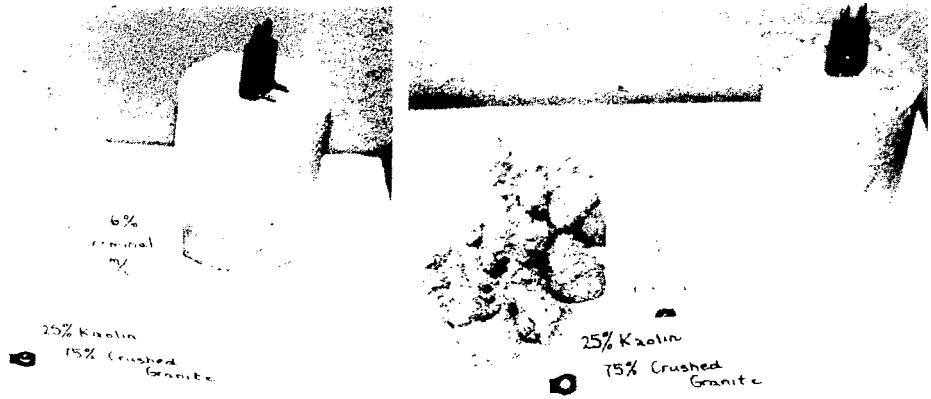

Crushed Granite + Kaolin
(75% + 25% mixes)

FIGURE 5: Specimens of Crushed Granite-Clay Mixtures Prepared by Standard Proctor Compaction

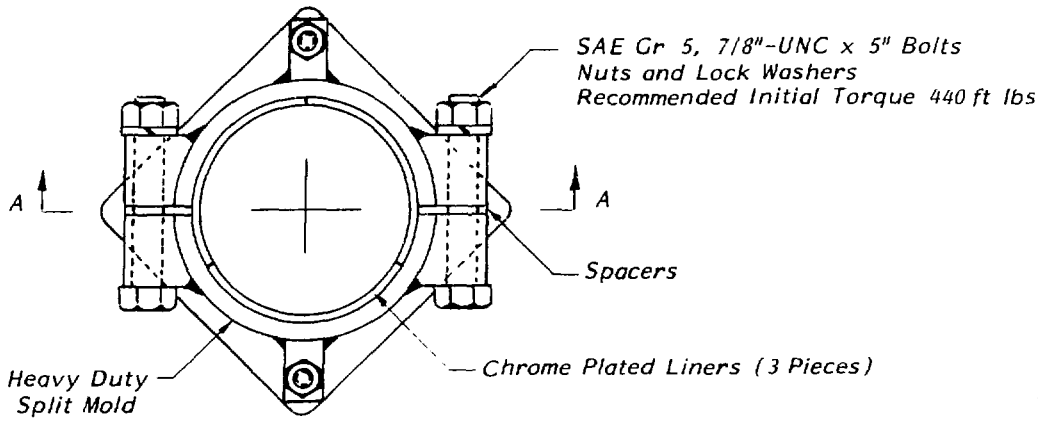

Top View

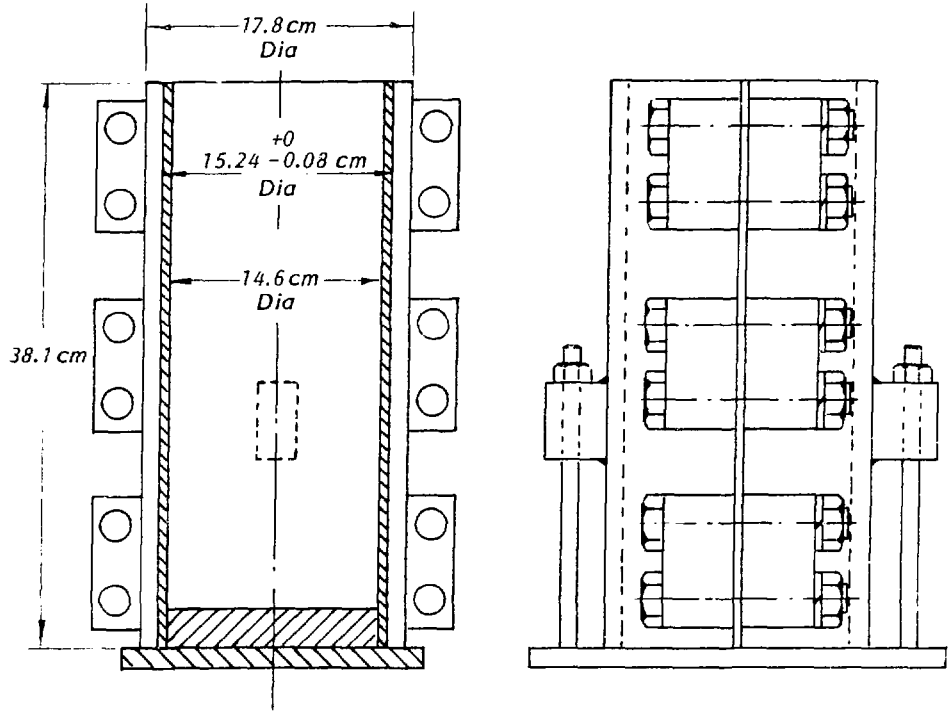

Sect A-A

Side View

FIGURE 6: Details of Static Compaction Mould

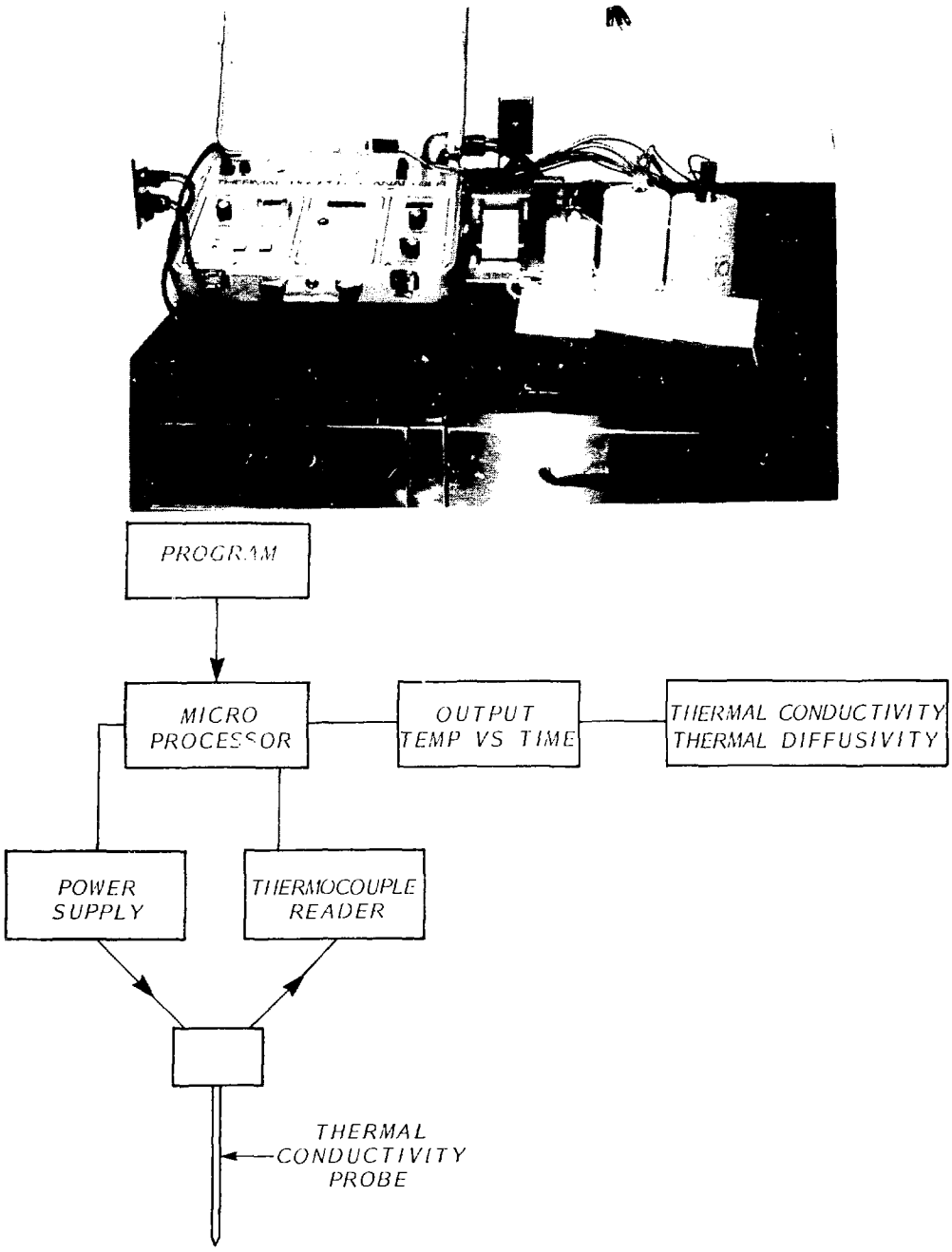

FIGURE 7: Transient Thermal Probe Technique for Measurement of Thermal Properties of Buffer Specimens

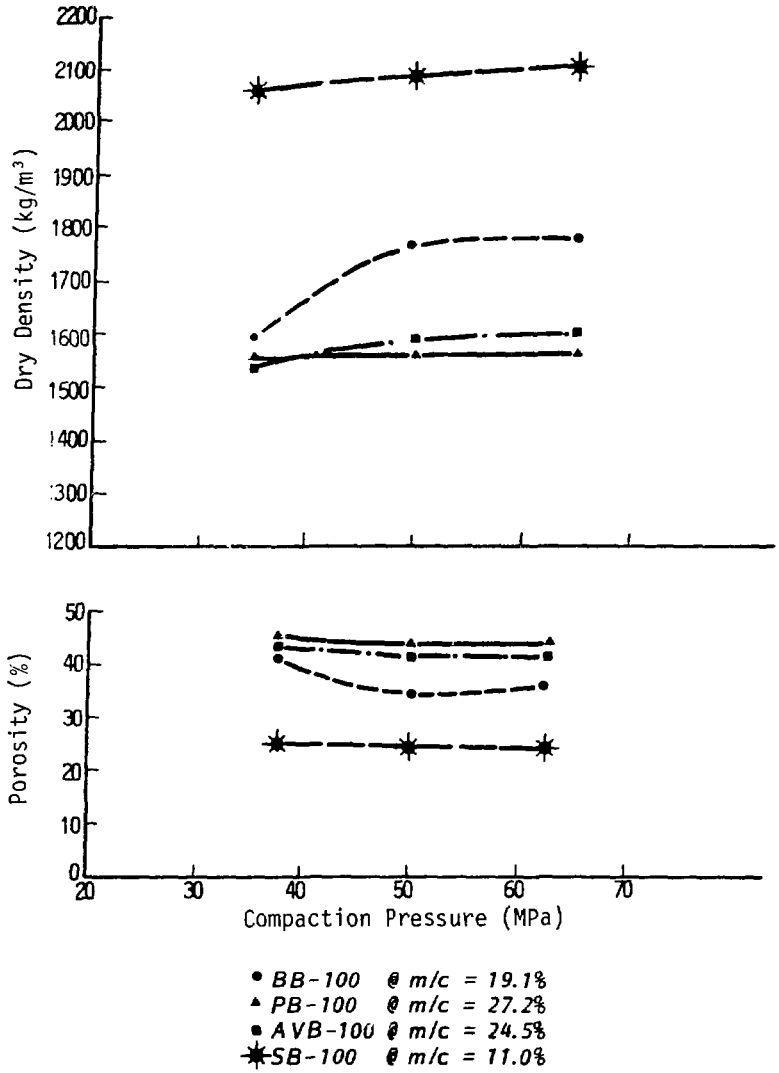

FIGURE 8: Correlation Between Sample Density/Porosity and Compaction Pressure for 100 Percent Clays (samples compacted in 100-mm Ø and 50-mm-high thick-walled stainless-steel moulds)

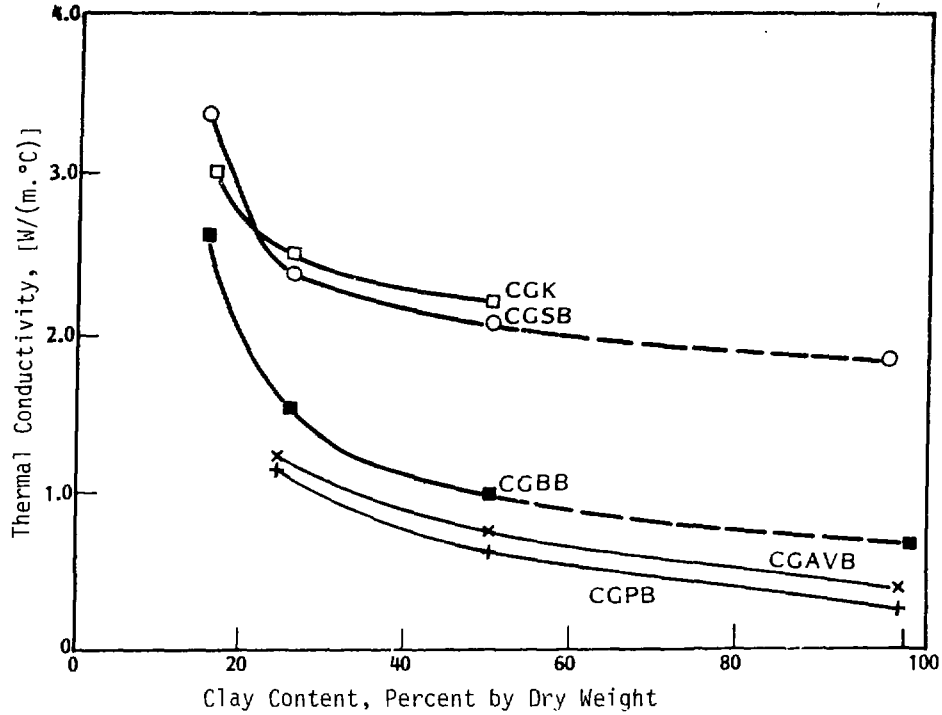

FIGURE 9: Thermal Conductivity as a Function of Clay Content in Crushed Granite and Clay Mixes

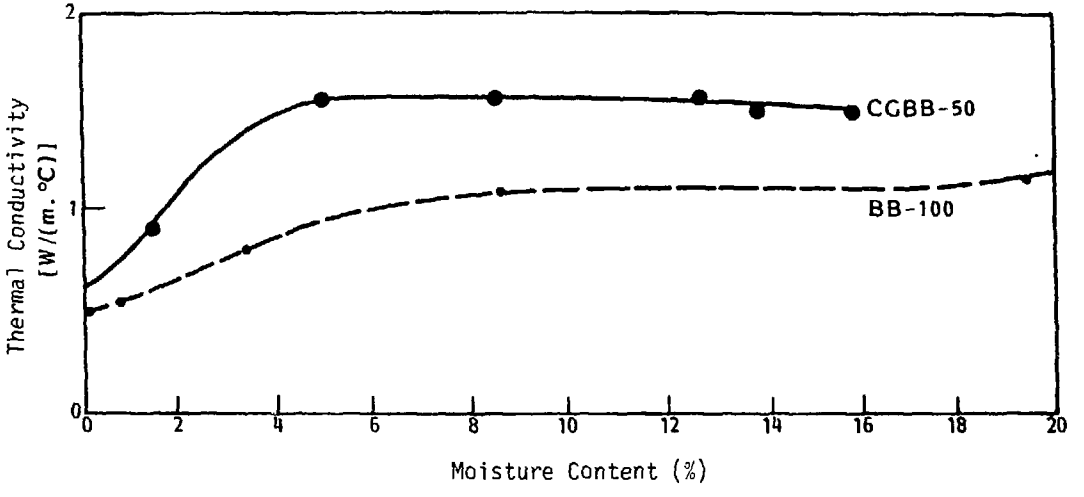

FIGURE 10: Thermal Conductivity vs. Moisture Content Relationship at Constant Density for Crushed Granite and Bentonite Buffer

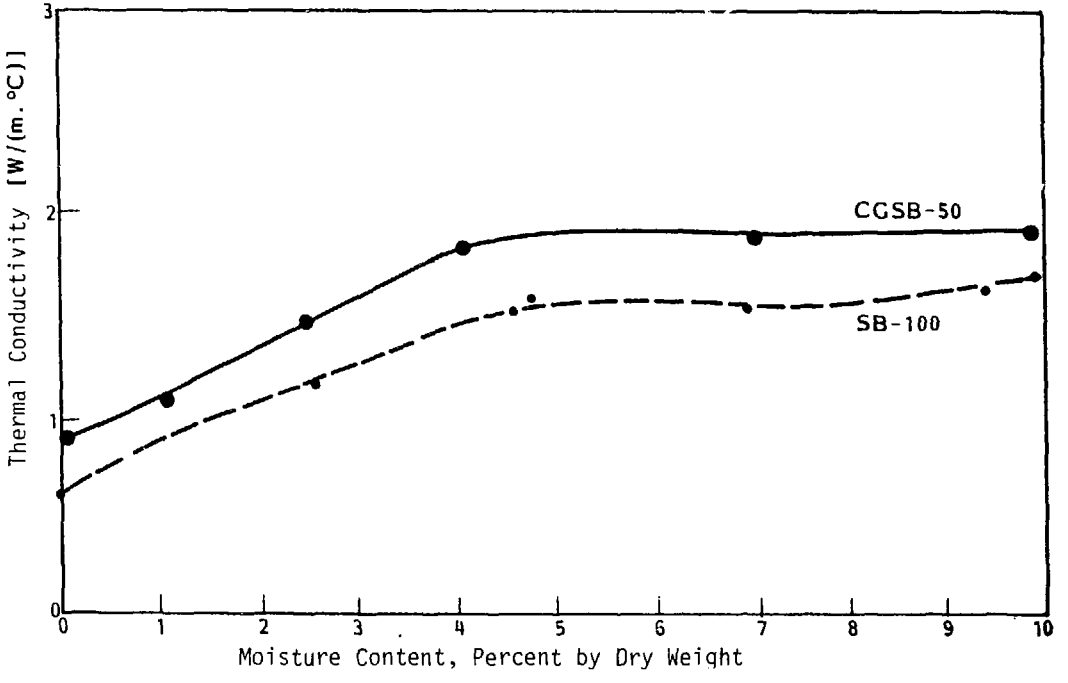

FIGURE 11: Thermal Conductivity vs. Moisture Content Relationship at Constant Density for Crushed Granite and Sealbond Buffer

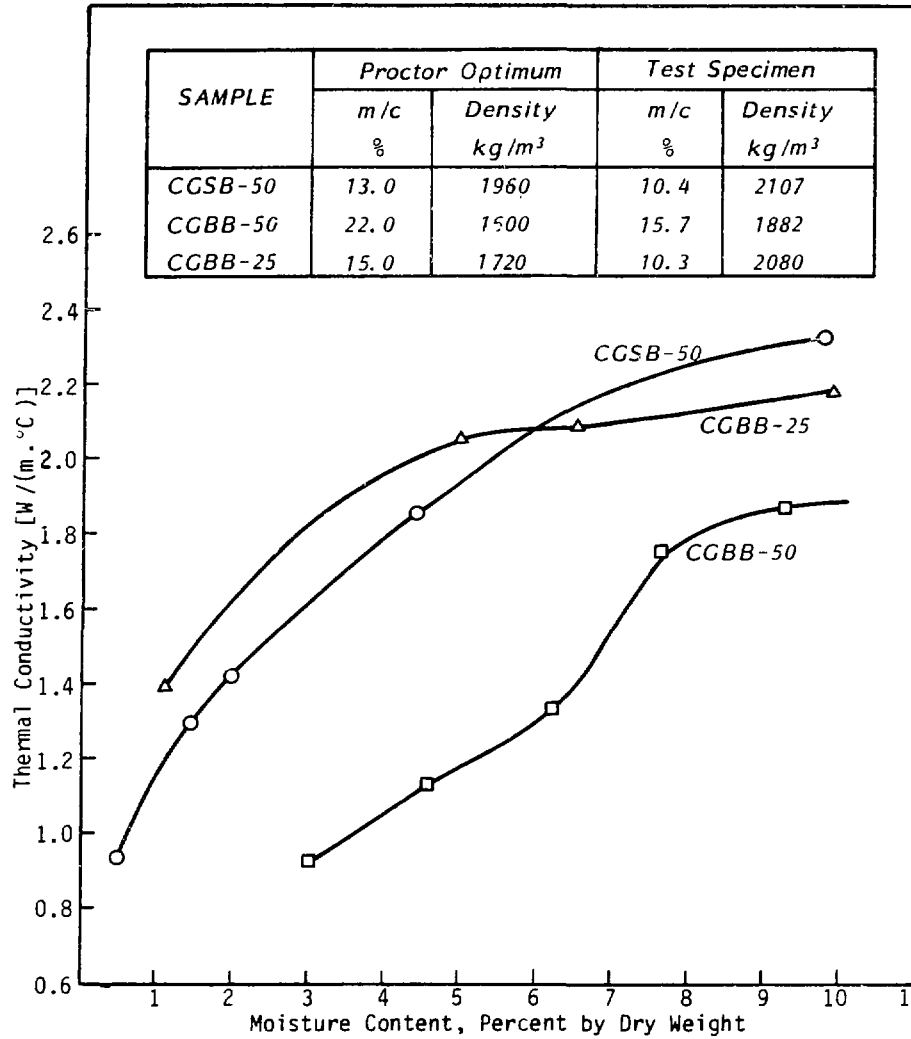

FIGURE 12: Thermal Conductivity vs. Moisture Content of Statically Compacted Crushed Granite and Clay Mixtures

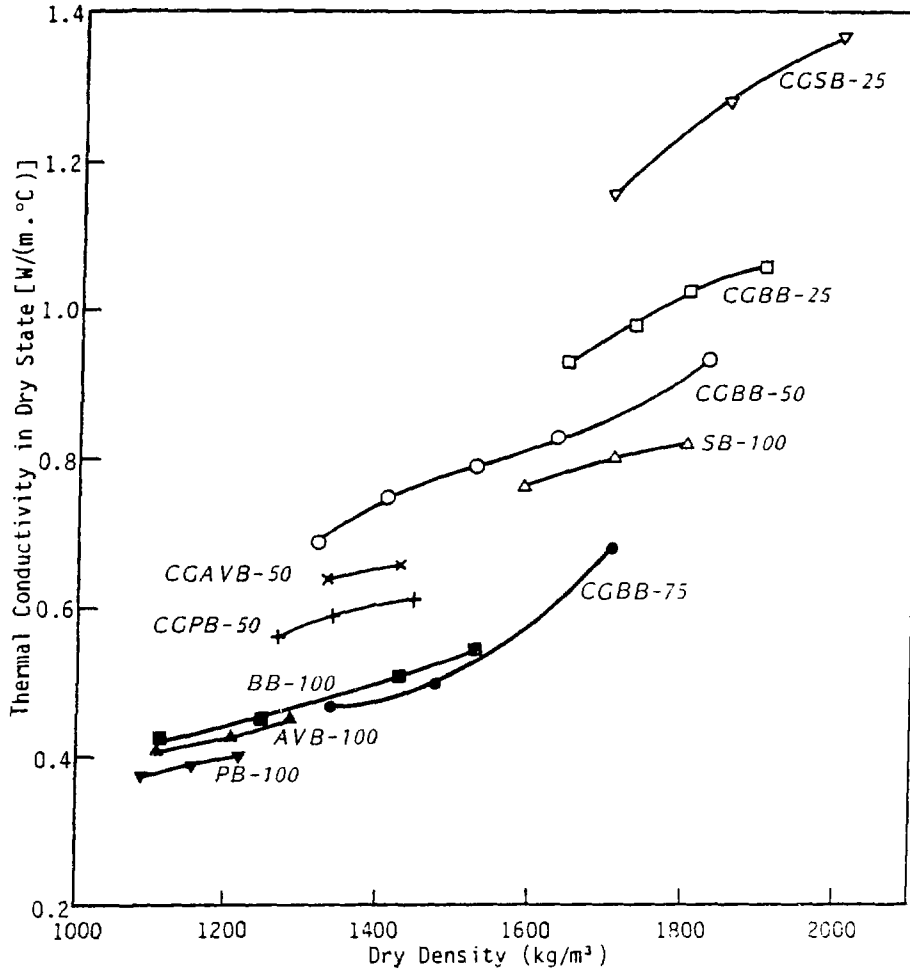

FIGURE 13: Dry Thermal Conductivity vs. Dry Density Relationship for Crushed Granite and Clay Mixes

TEST MOULD AND COMPACTED SAMPLE FOR HIGH TEMPERATURE THERMAL CONDUCTIVITY TEST

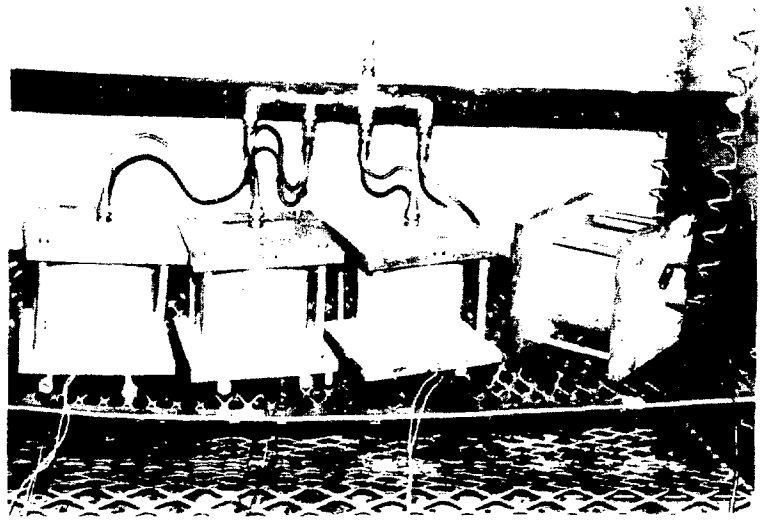

FIGURE 14: Test Arrangement for Thermal Conductivity Measurement of Compacted Samples at High Temperatures

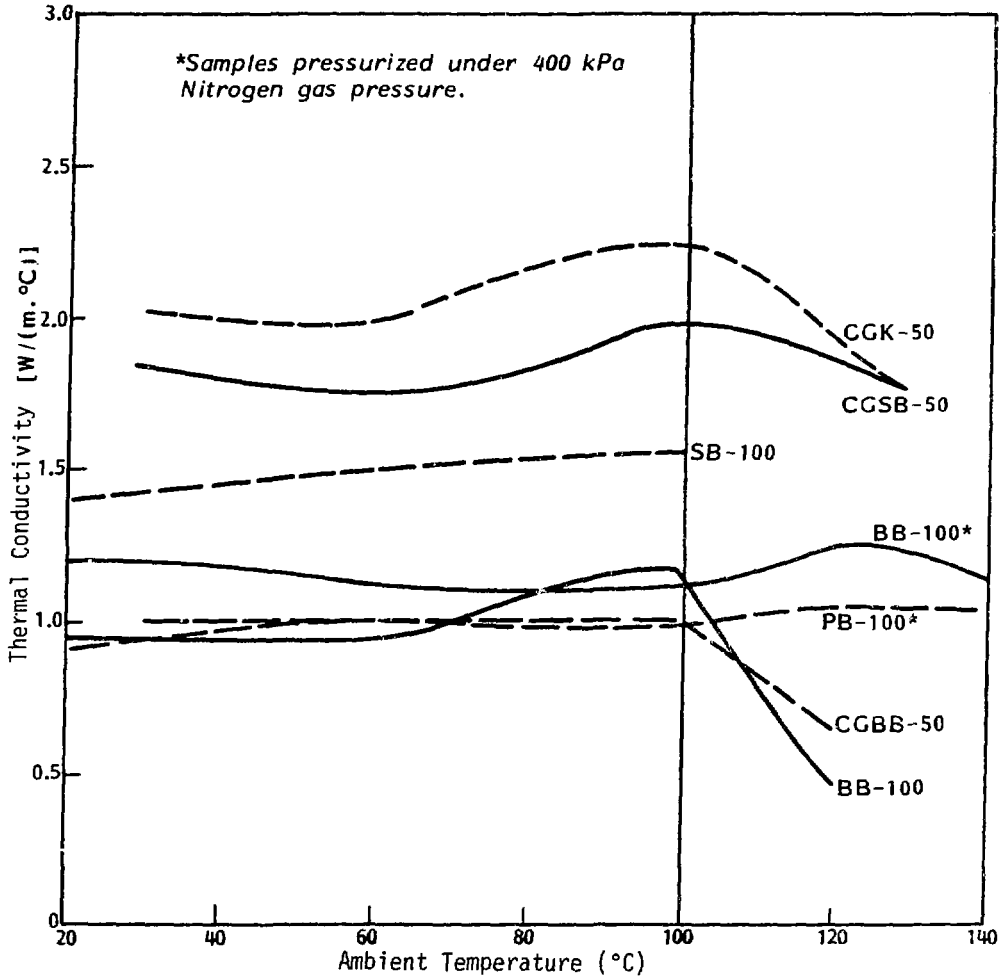

FIGURE 15: Thermal Conductivity as a Function of Ambient Temperature

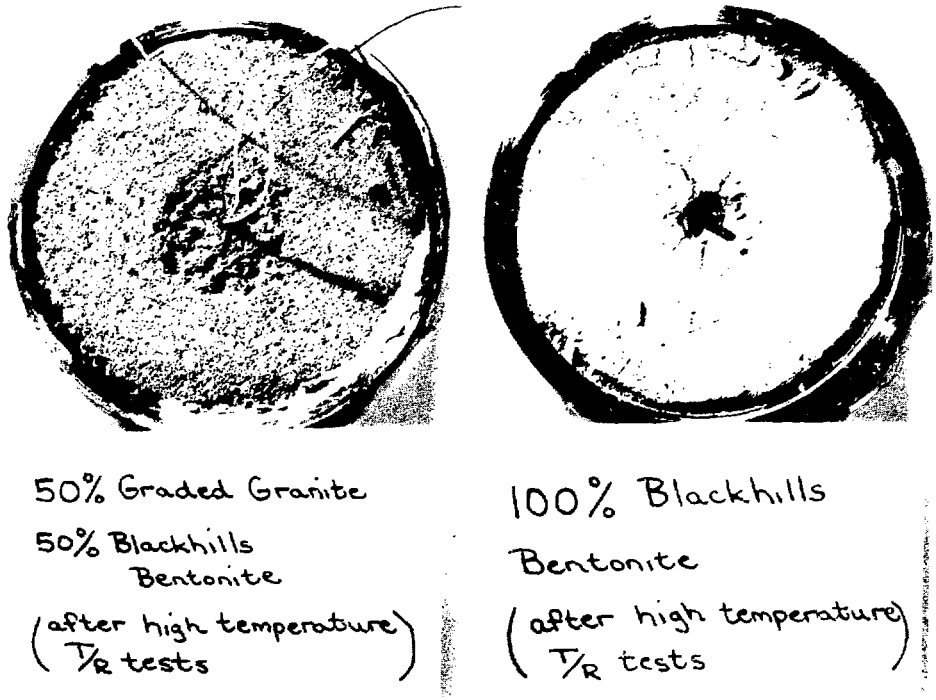

FIGURE 16: Shrinkage and Cracking of Moisture-Sealed Samples after Subjecting to High Temperature (120°C)

Sealed sample and pressurized.

Note the shrinkage but no cracking.

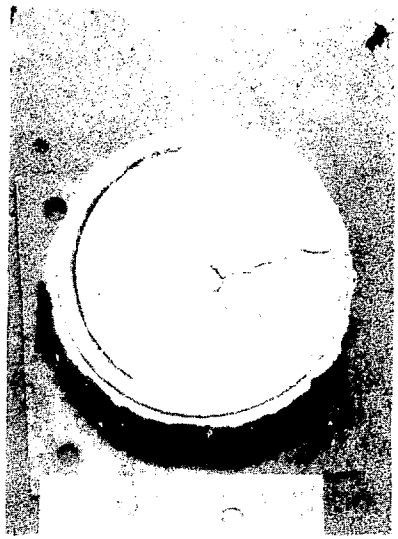

Sealed sample but not pressurized.

Note the shrinkage and cracking due to moisture loss.

FIGURE 17: Sample Condition after High-Temperature (125°C) Test (Black Hills bentonite compacted to 1300 kg/m^3 at 20% moisture content)

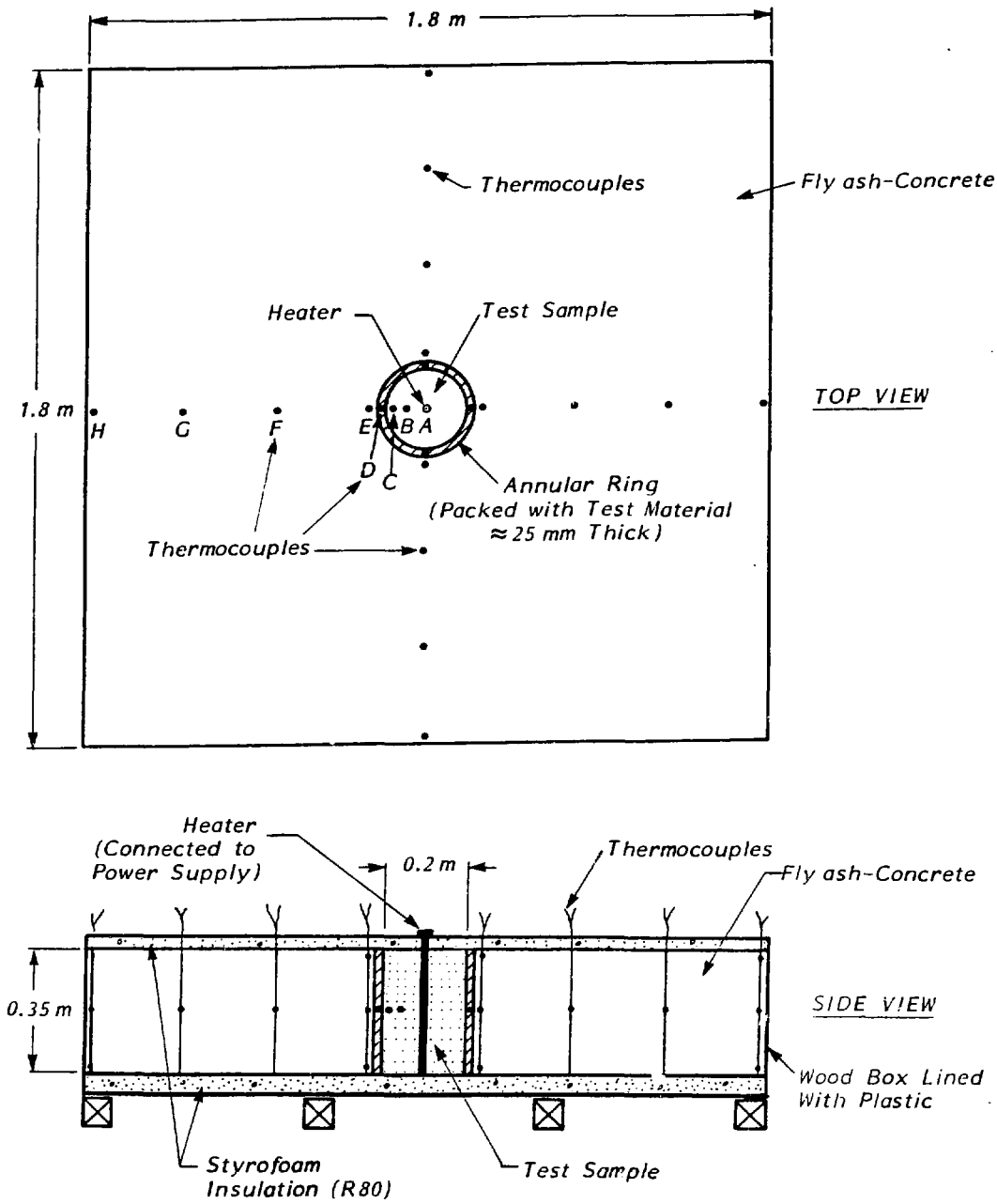

FIGURE 18: Schematic of Heater Experiment for Compacted Buffer Samples

CCBB 50

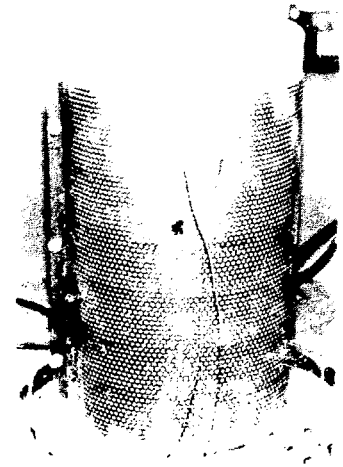

BB 100

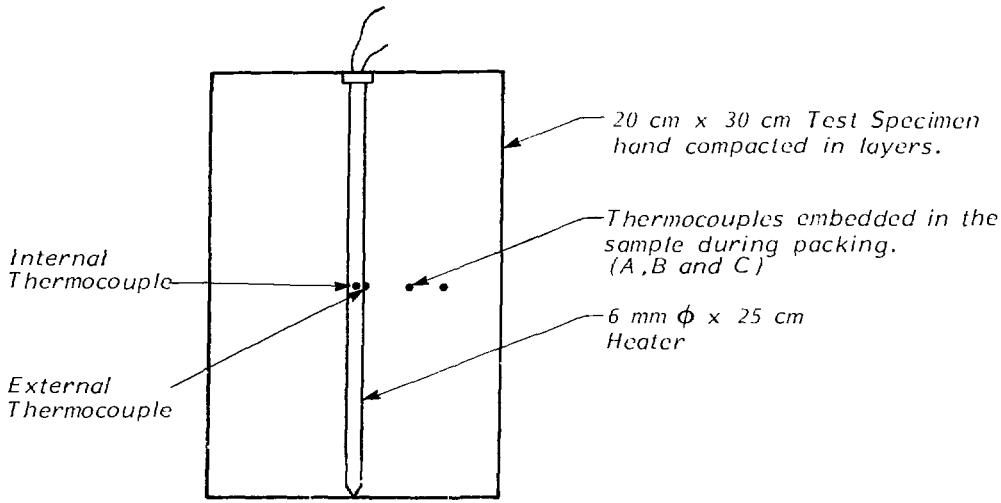

FIGURE 19: Compacted Test Sample for Heater Experiment

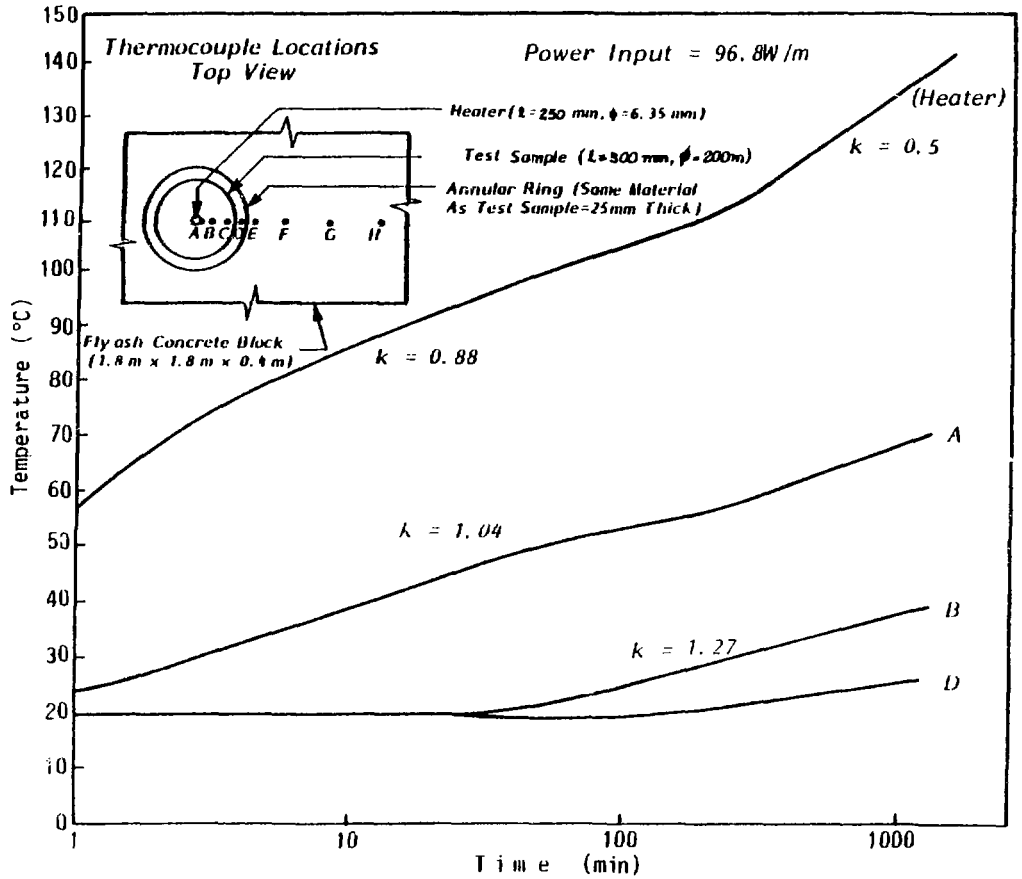

FIGURE 20: Heater Test - Black Hills Bentonite Samples (Dry Density = 1476 kg/m^3; Initial Moisture Content = 19.1%)

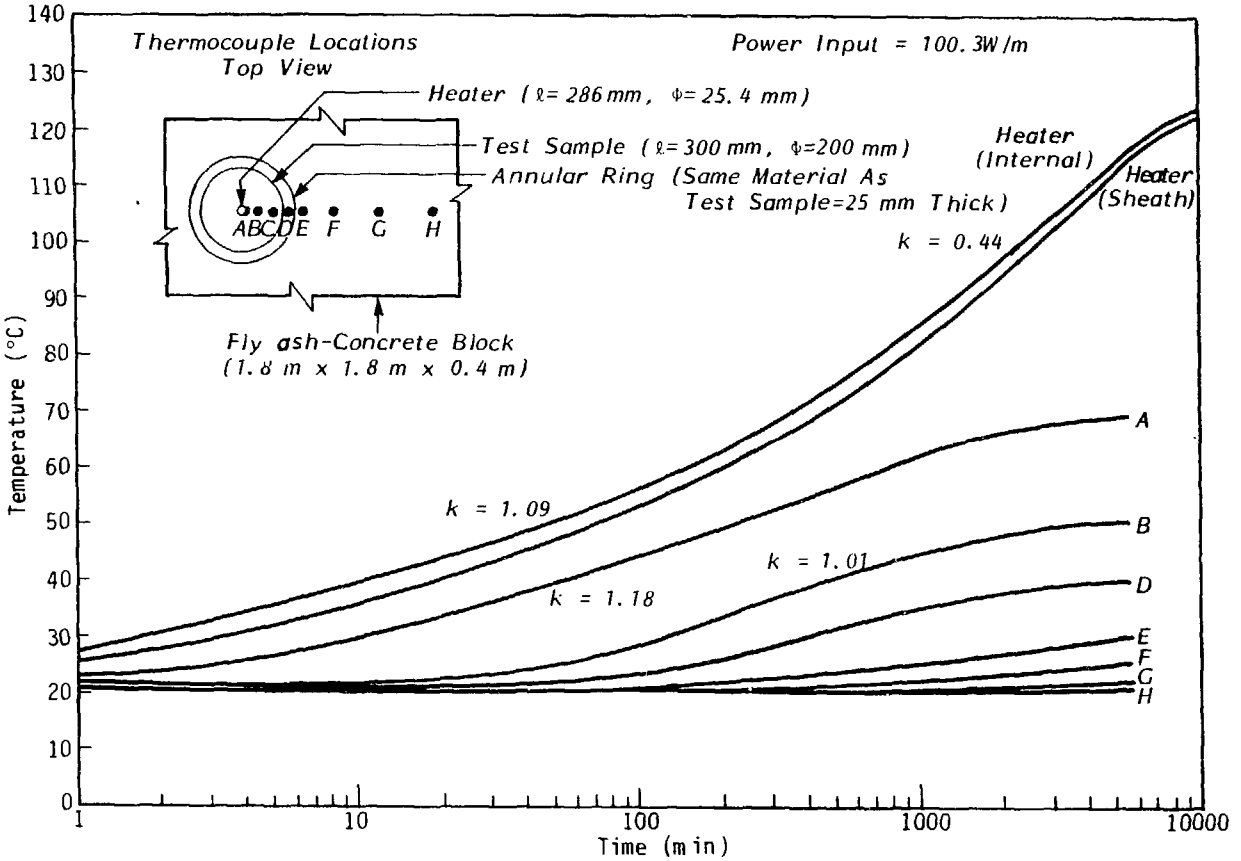

FIGURE 21: Heater Test - Black Hills Bentonite (Dry Density = 1426 kg/m^3; Initial Moisture Content = 19.9%)

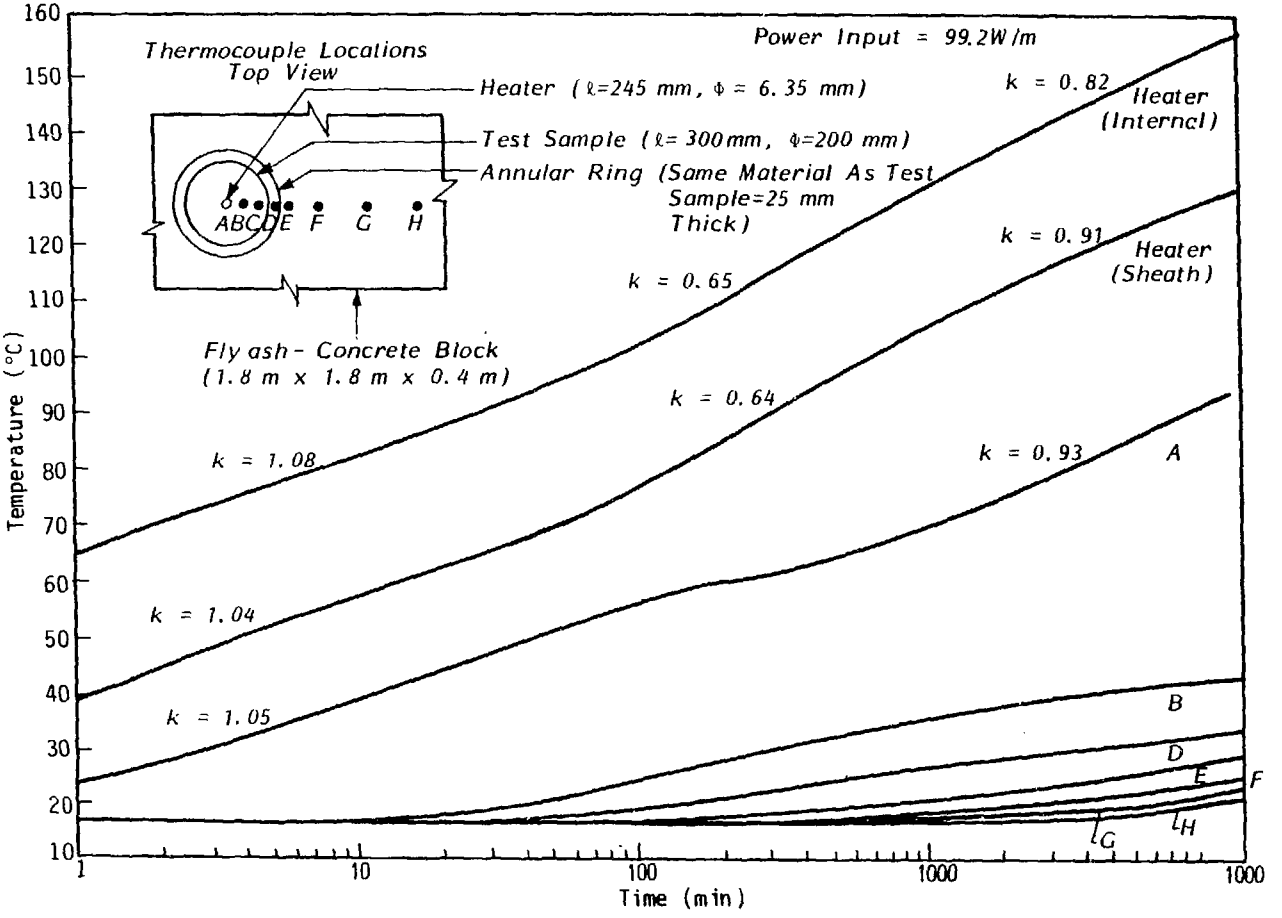

FIGURE 22: Long-Term Heat Test - 50% Crushed Granite + 50% Black Hills Bentonite (Dry Density = 1440 kg/m^3; Initial Moisture Content = 13.9%)

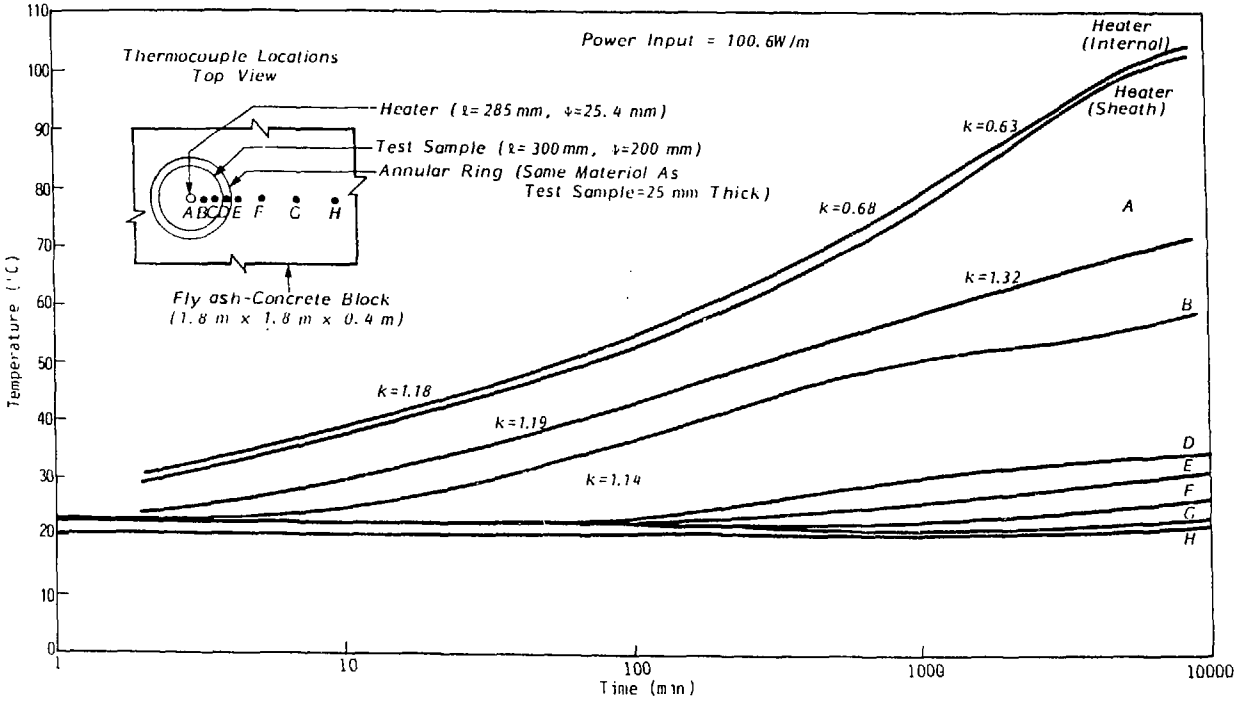

FIGURE 23: Long-Term Heater Test - 50% Crushed Granite + 50% Black Bentonite (Dry Density = 1495 kg/m^3; Initial Moisture Content = 14.0%)

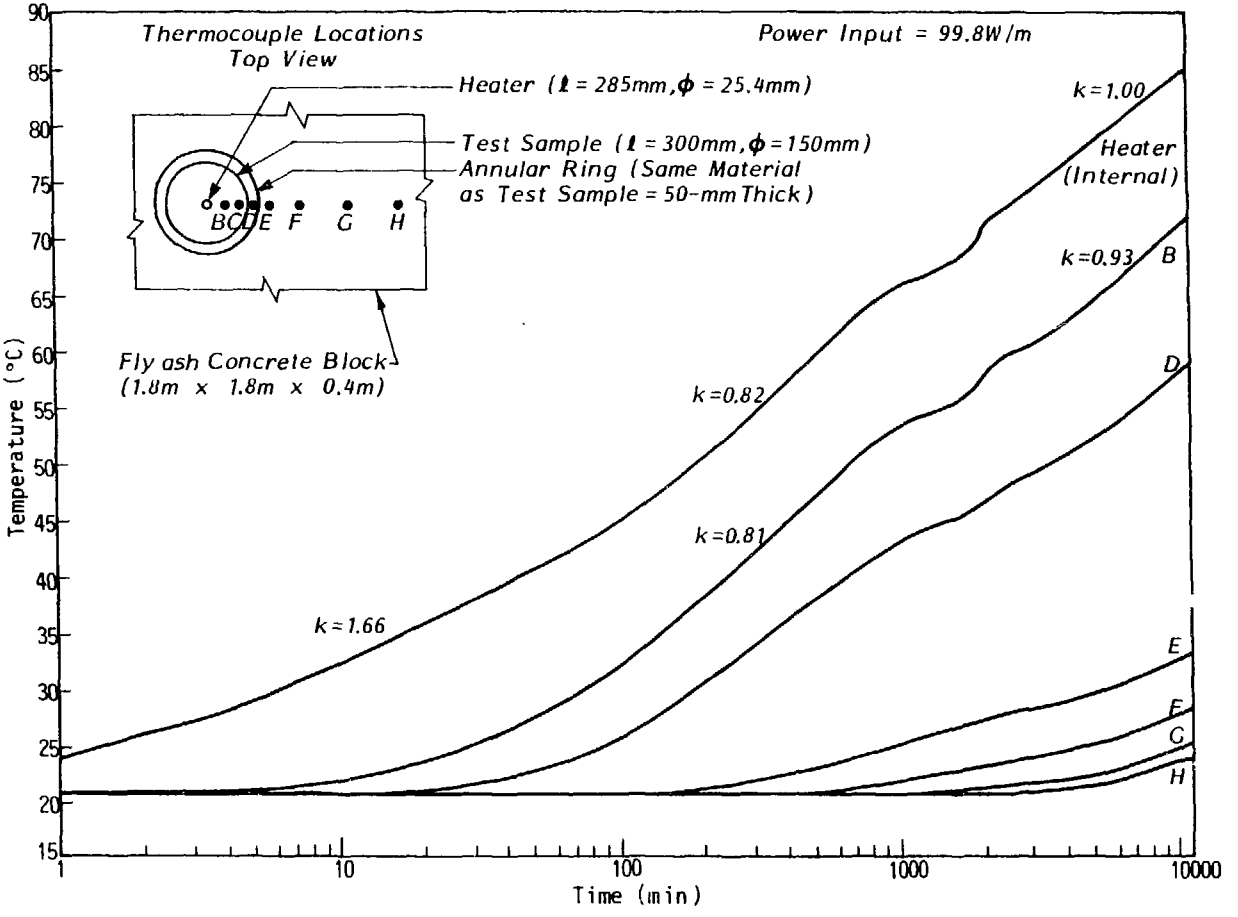

FIGURE 24: Heater Test - Black Hills Bentonite (Statically Compacted) (Dry Density = 1555 kg/m^3; Initial Moisture Content = 20%)

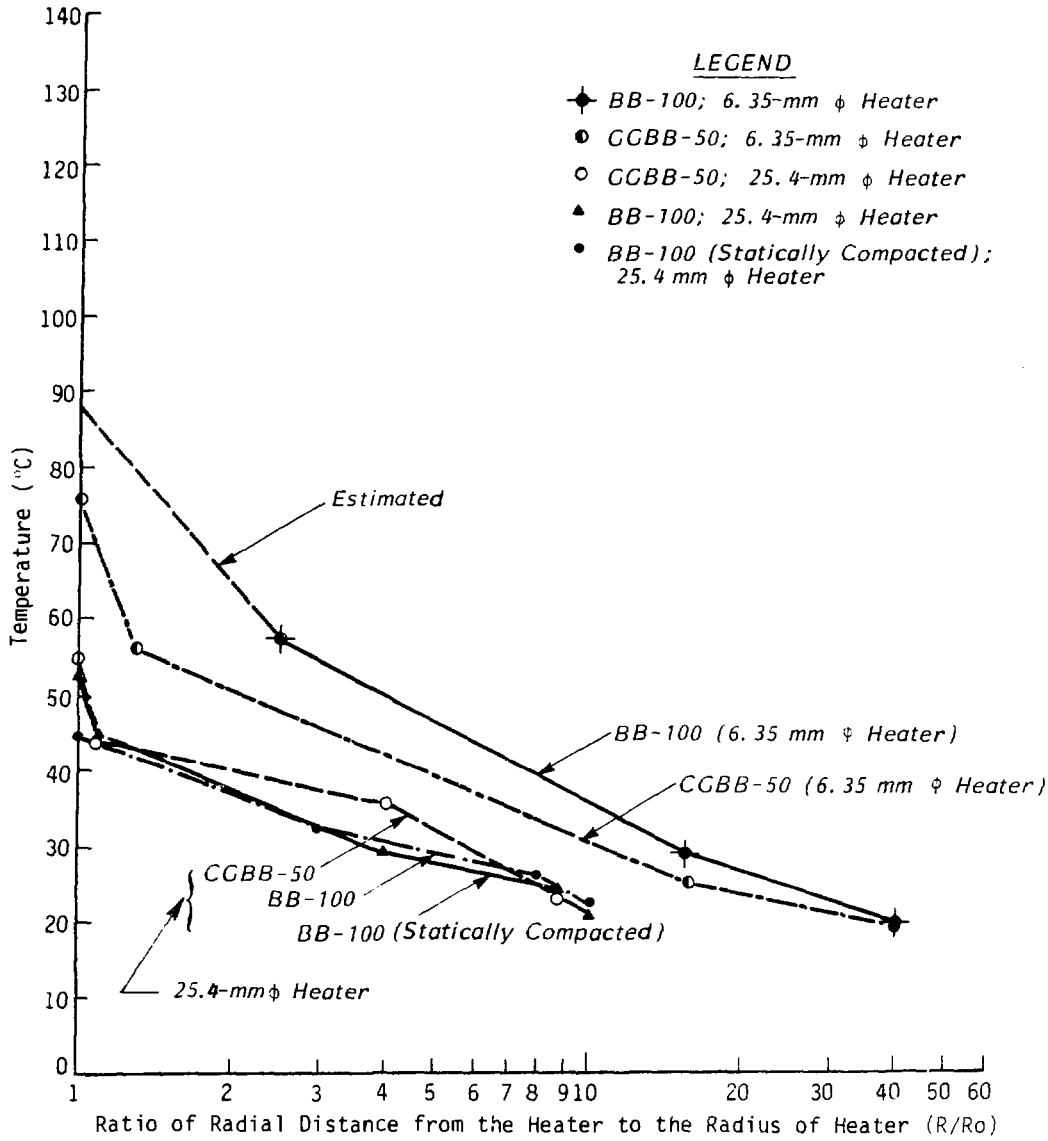

FIGURE 25: Plot Showing Temperature Profile at Initial Drying Time

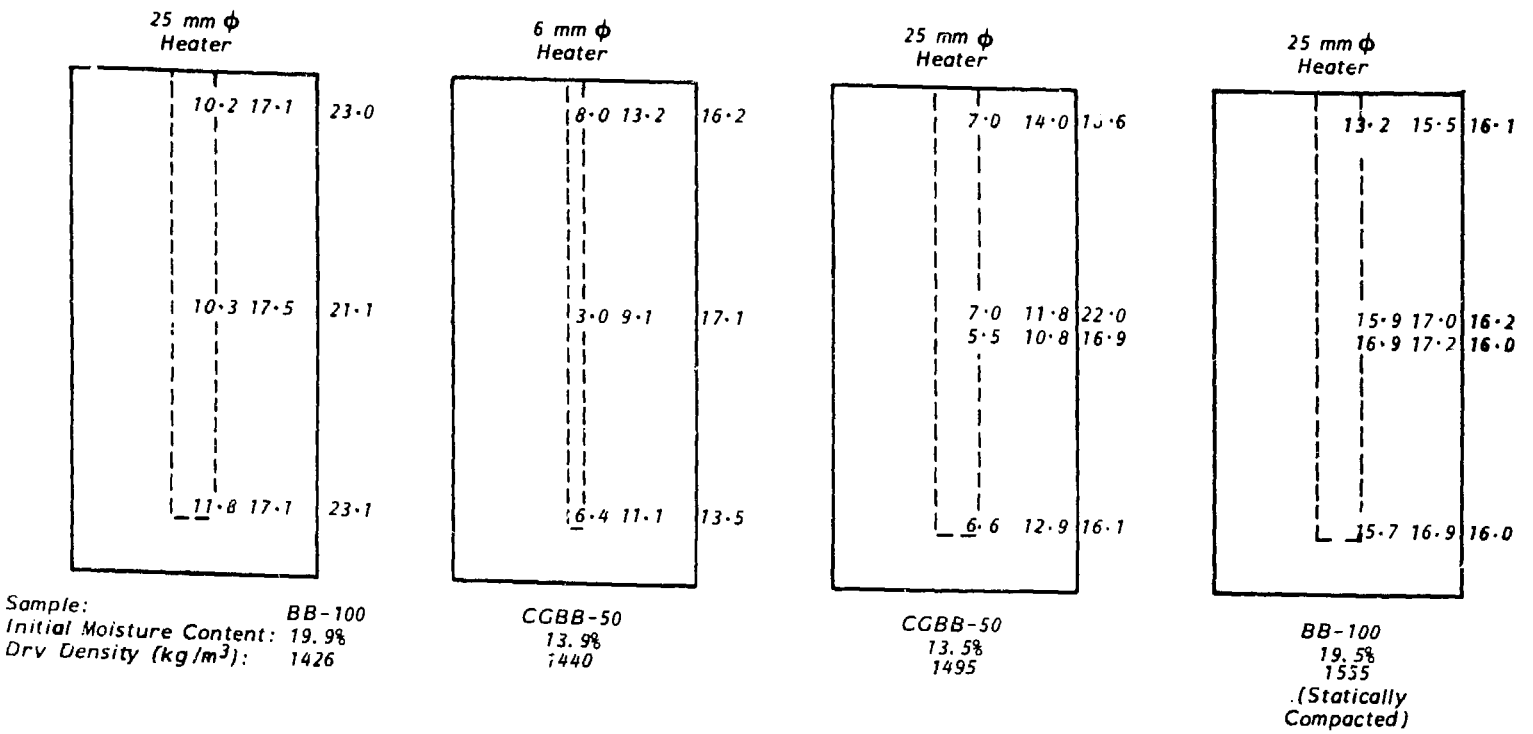

FIGURE 26: Distribution of Moisture Content after Heater Test

FIGURE 27: Black Hills Bentonite Sample after 7 Days of Heater Test. (Note the local thermal drying and shrinkage cracks around 6 mm ∅ heater.)

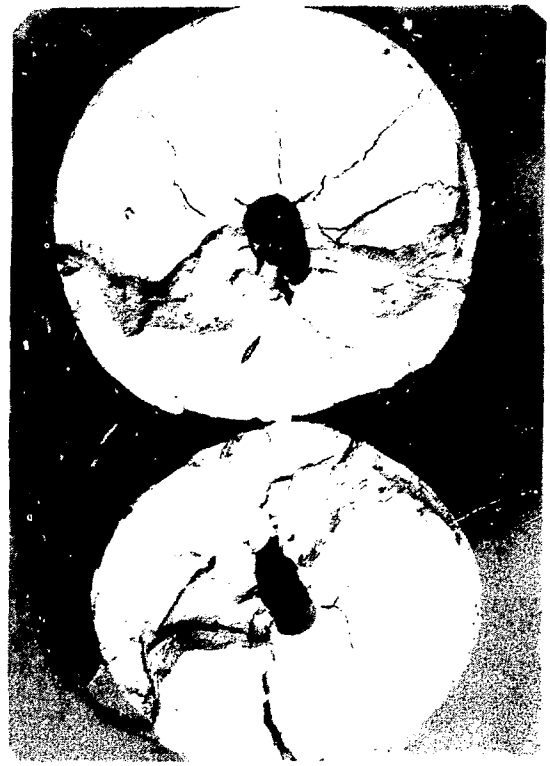

FIGURE 28: 100% Black Hills Bentonite Samples after 7 Days of Heater Test (Note the severe cracking around 25 mm Ø heater)

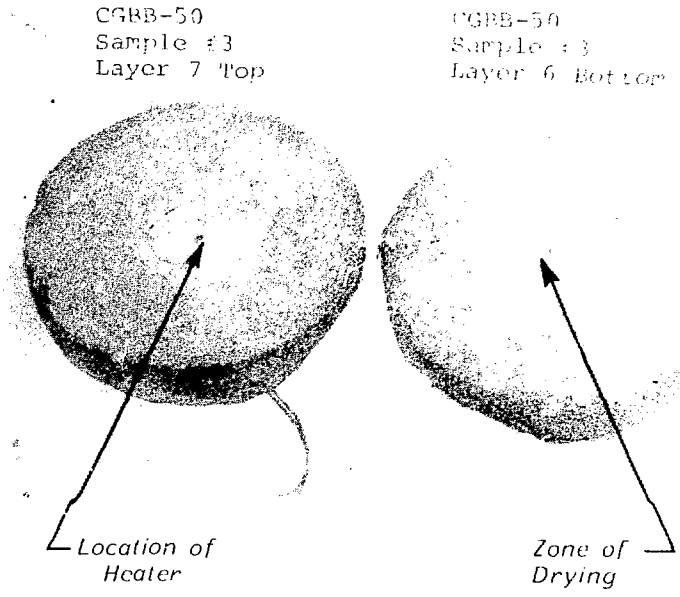

FIGURE 29: Crushed Granite and Black Hills Bentonite Sample after 7 Days of Heater Test (Note the zone of thermal drying but no cracking around 6.3 mm Ø heater)

FIGURE 30: Crushed Granite and Black Hills Bentonite Samples after 7 Days of Heater Test. (Note the zone of thermal drying with moderate cracking around 25 mm Ø heater)

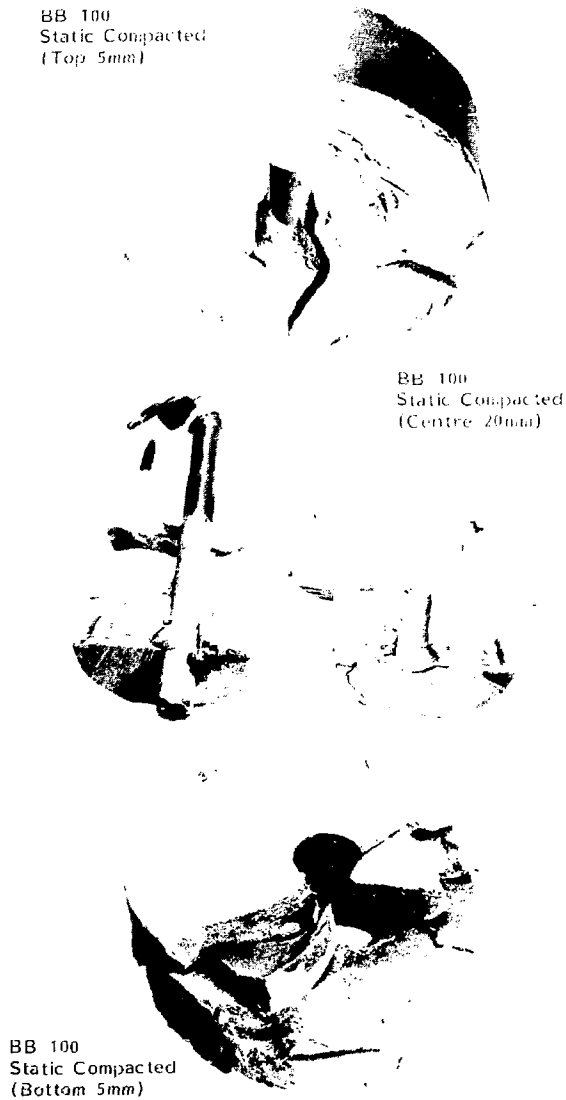

FIGURE 31: Black Hills Bentonite Sample (static compaction) After Seven Days of Heater Test (Note sample was sawn apart horizontally, but broke along vertical hairline cracks) 25 mm Ø Heater

ISSN 0067-0367

To identify individual documents in the series we have assigned an AECL- number to each.

Please refer to the AECL- number when requesting additional copies of this document from

Scientific Document Distribution Office
Atomic Energy of Canada Limited
Chalk River, Ontario, Canada
KOJ 1JO

Price: $4.00 per copy

ISSN 0067-0367

Pour identifier les rapports individuels faisant partie de cette série nous avons assigné un numéro AECL- à chacun.

Veuillez faire mention du numéro AECL -si vous demandez d'autres exemplaires de ce rapport au

Service de Distribution des Documents Officiels
L'Energie Atomique du Canada Limitée
Chalk River, Ontario, Canada
KOJ 1JO

prix: $4.00 par exemplaire